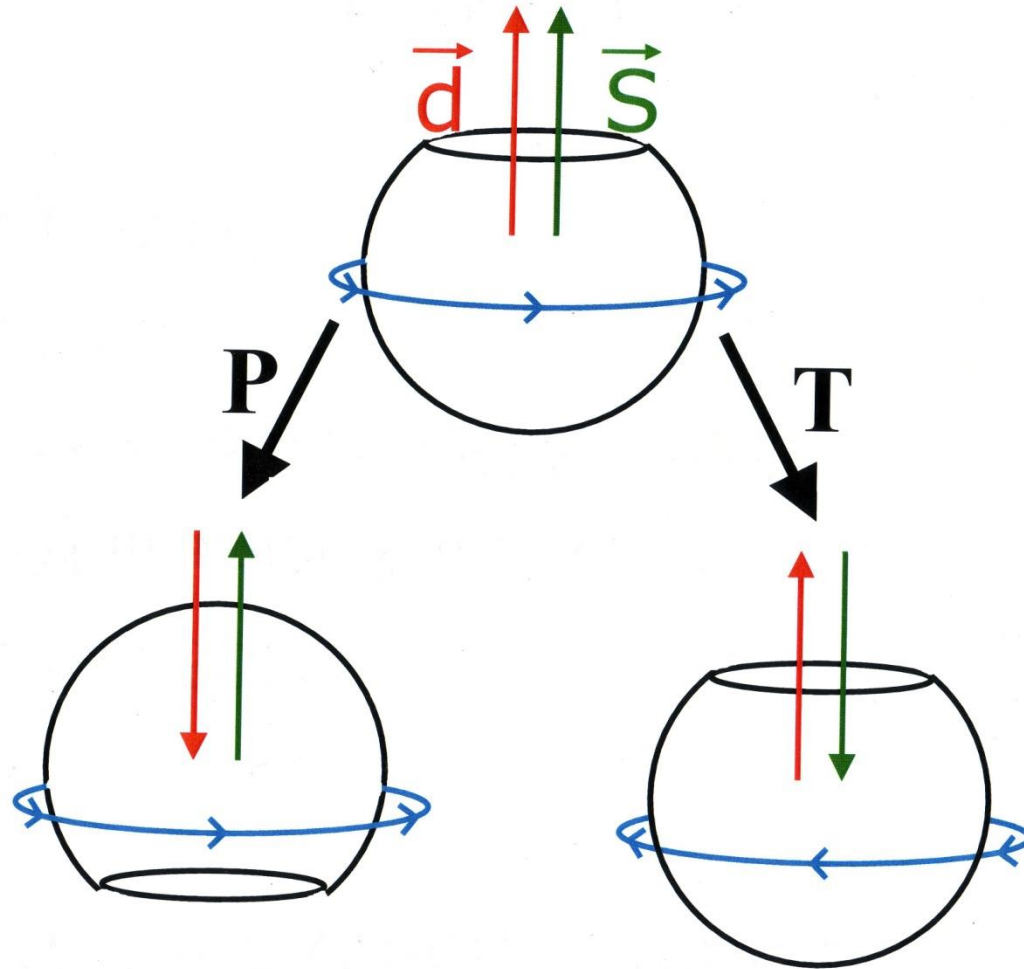


An EDM Violates P and T

Purcell
Ramsey
Landau

$$H_{\text{Magnetic dipole}} = -\vec{\mu} \cdot \vec{B} = -\mu\vec{\sigma} \cdot \vec{B} \quad H_{\text{Electric dipole}} = -\vec{d} \cdot \vec{E} = -d\vec{\sigma} \cdot \vec{E}$$



CPT theorem \Rightarrow T-violation = CP-violation

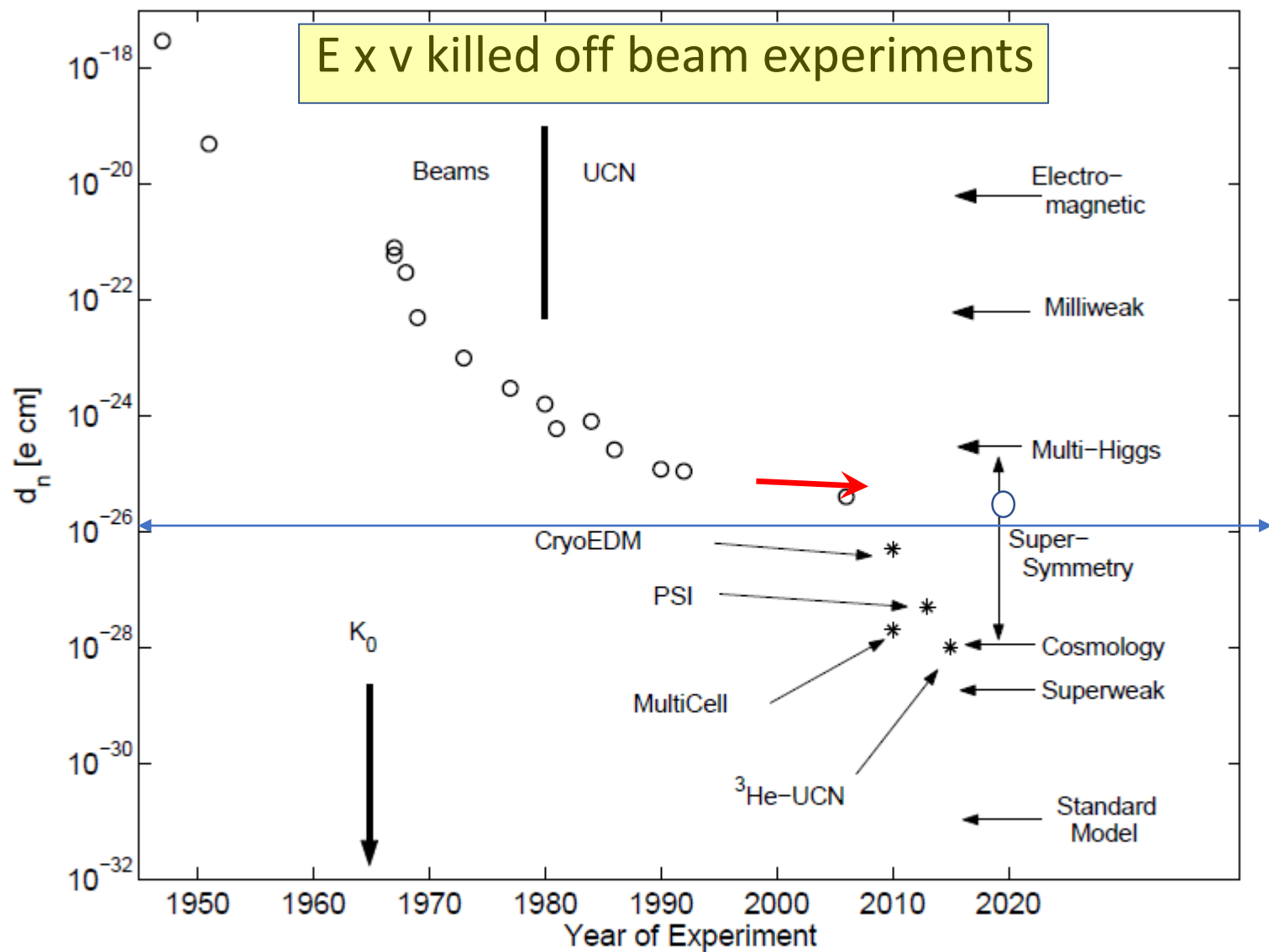
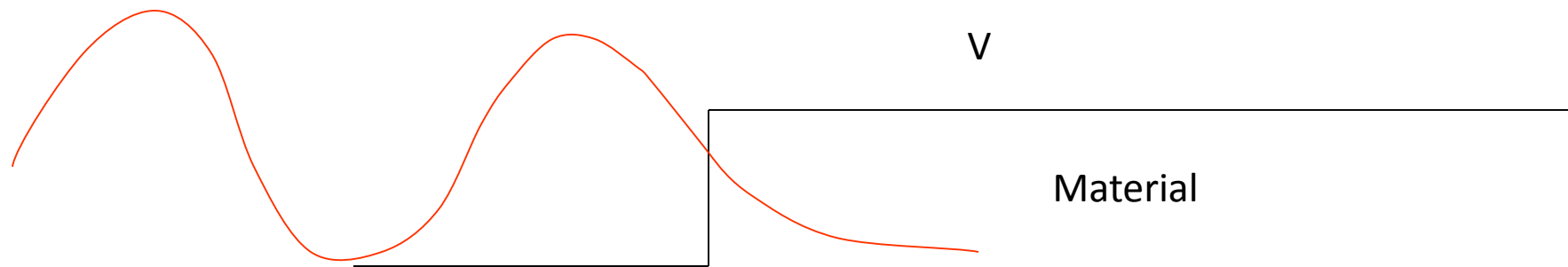


Fig. 1. Historical development of the neutron EDM experimental limit along with expectations from various theoretical models. The points marked with * are experiments presently under development or proposed, and will be discussed in this review.

Ultra-Cold Neutrons (UCN)

- $E < V_c$ critical energy for total reflection
- UCN totally reflected for all angles of incidence

$$E \sim 10^2 \text{ neV} \quad \lambda \sim 500 \text{ \AA} \quad T \sim 1 \text{ mK} \quad h \sim 1 \text{ m} \quad (mgh \sim E)$$
$$B \sim 2 \text{ Tesla} \quad (\mu B \sim E)$$



Wave fn penetrates material -> wall losses limit storage time

Need for a co-magnetometer

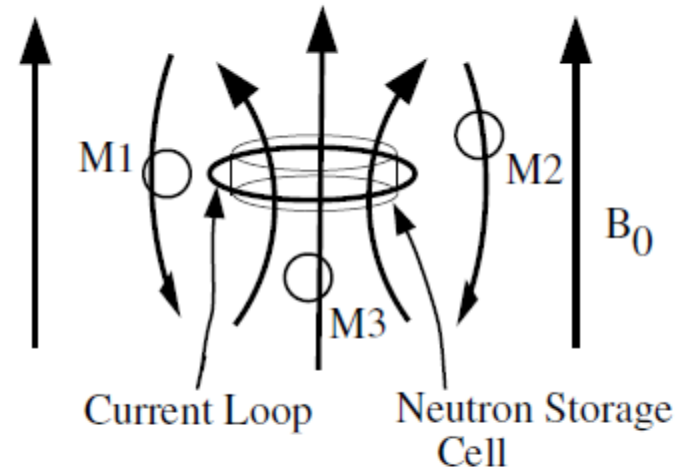


Fig. 3. The external magnetometer problem. Leakage currents associated with the application of a high voltage to the measurement cell can flow in a loop (or some fraction thereof) around the cell, creating a magnetic field that is correlated with the direction of the electric field. Depending on the location of a magnetometer, the field from the loop can add or subtract to the applied static field B_0 .

What is Unique About Our Experiment



- Production of ultracold neutrons (UCN) within the apparatus
 - *higher UCN density and longer storage times*
- Use of liquid as a high voltage insulator
 - *higher electric fields*
- Use of a ^3He co-magnetometer and superconducting shield
 - *better control of magnetic field systematics*
- Employ two different measurement techniques
 - *oscillation of scintillation rate and dressed spin techniques*

Tackling unknown systematic effects requires unique handles in the experiment that can be varied.

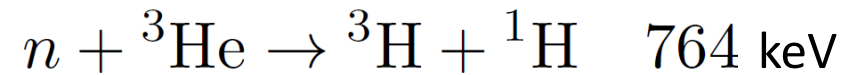


Polarized He3 as:

- Polarizer (partial..beam is polarized
- Magnetometer
- Analyzer
- Detector

Signal in the SNS nEDM Experiment

- Neutron interaction with ^3He is spin dependent



- Interaction is spin dependent, sensitivity to the angle between the neutron and ^3He

$$S(t) = \frac{\rho_{UCN} V}{\tau_{^3\text{He}}} (1 - P_n P_{^3\text{He}} \cos \theta_{n^3}(t))$$

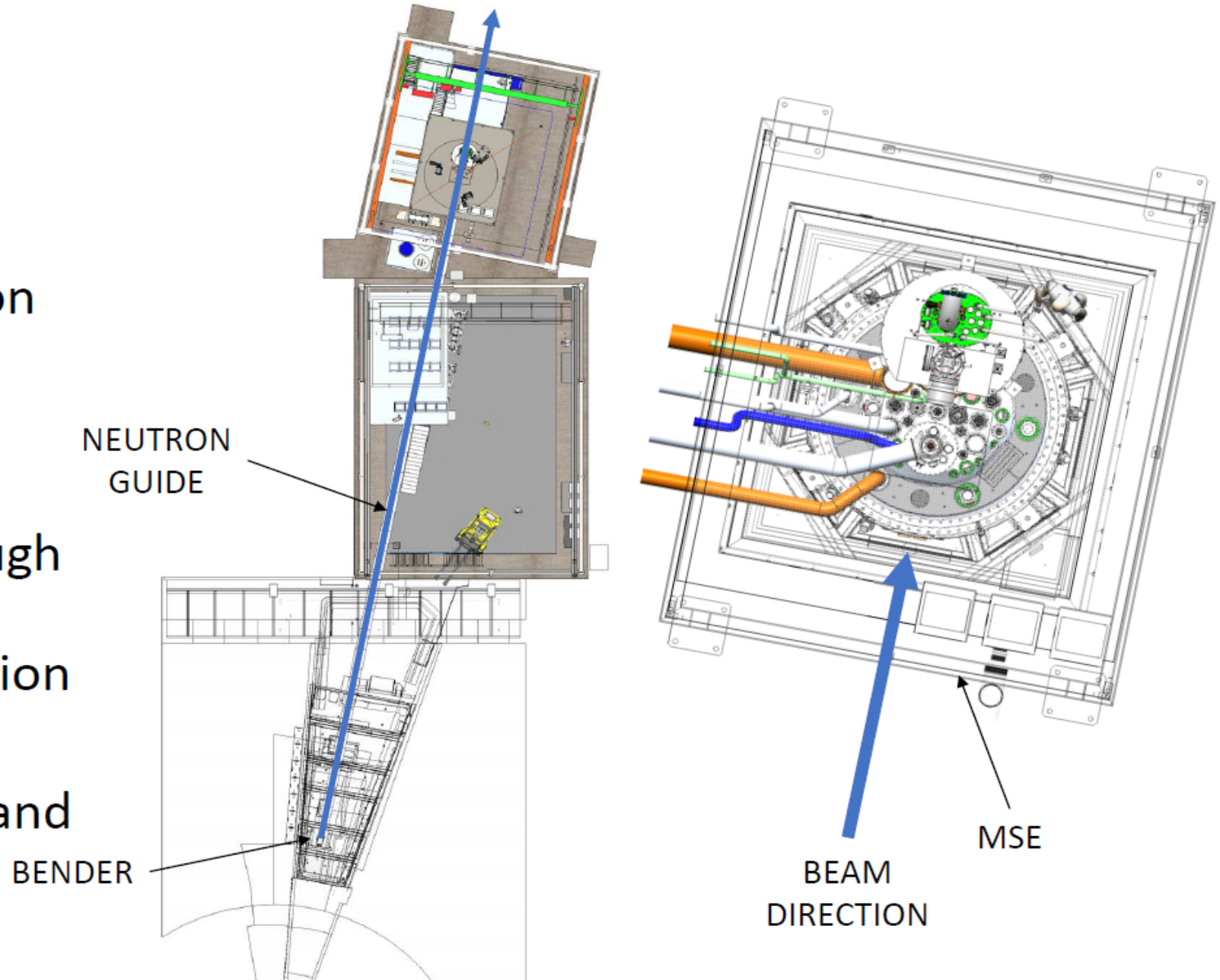

 $\langle \sigma_n \cdot \sigma_3 \rangle$

$$\Delta\theta_{\pm} = \frac{4d_n ET}{\hbar}$$



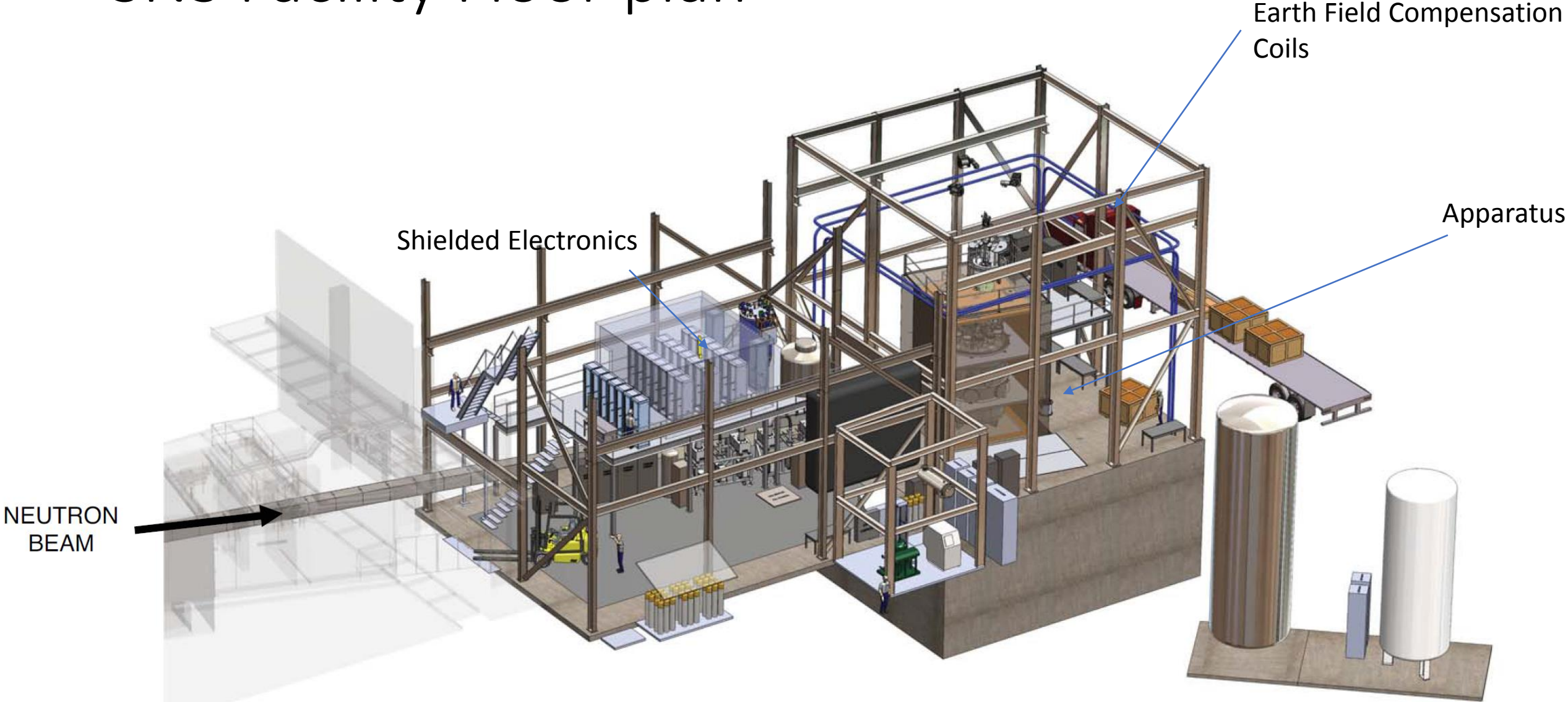
Beamline

- The beamline direction from the bender
- Preference for beam guide passing perpendicularly through the magnetic shield dictates MSE orientation
- Building should be aligned with the FCS and MSE



SNS Facility Floor plan

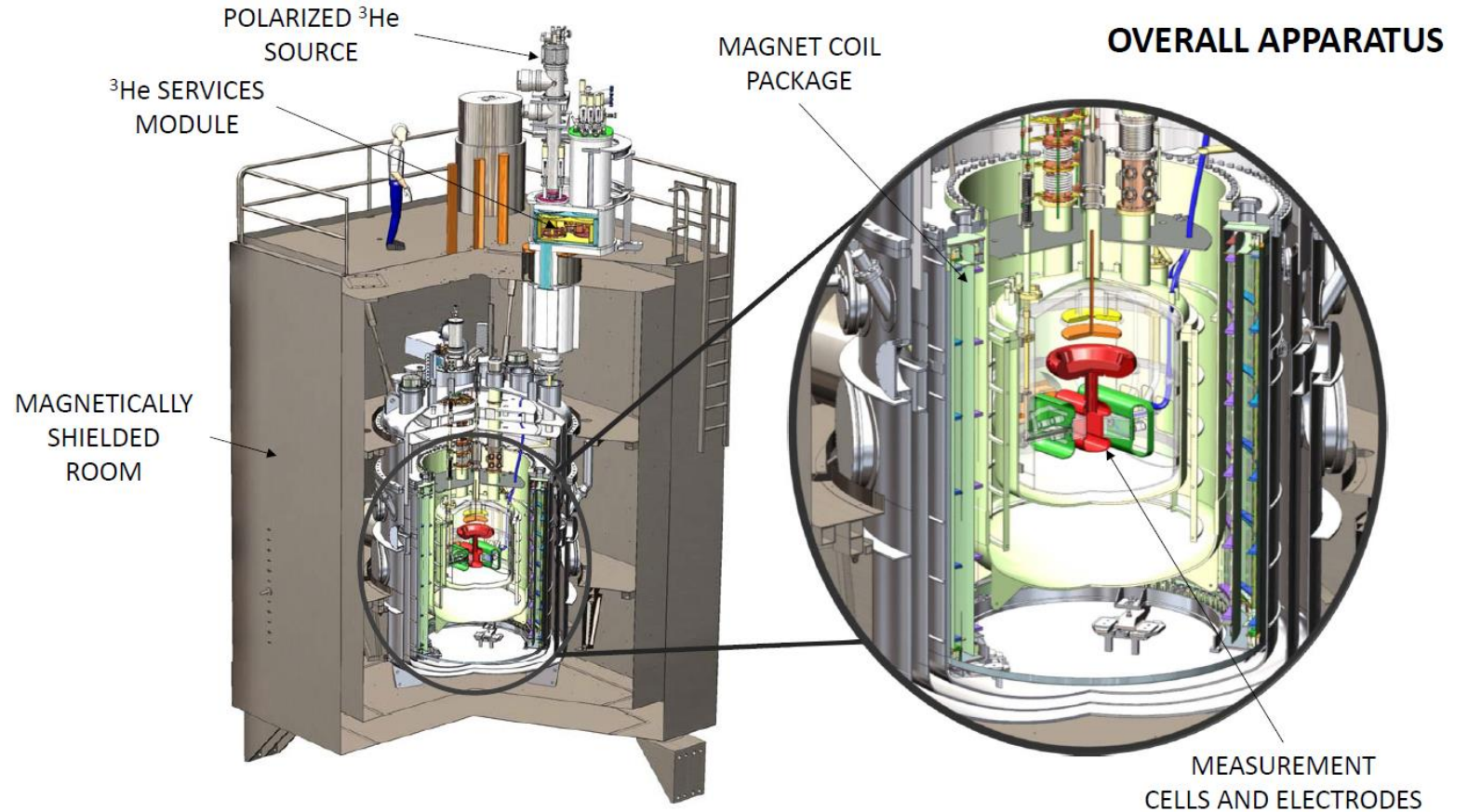
Chris Swank

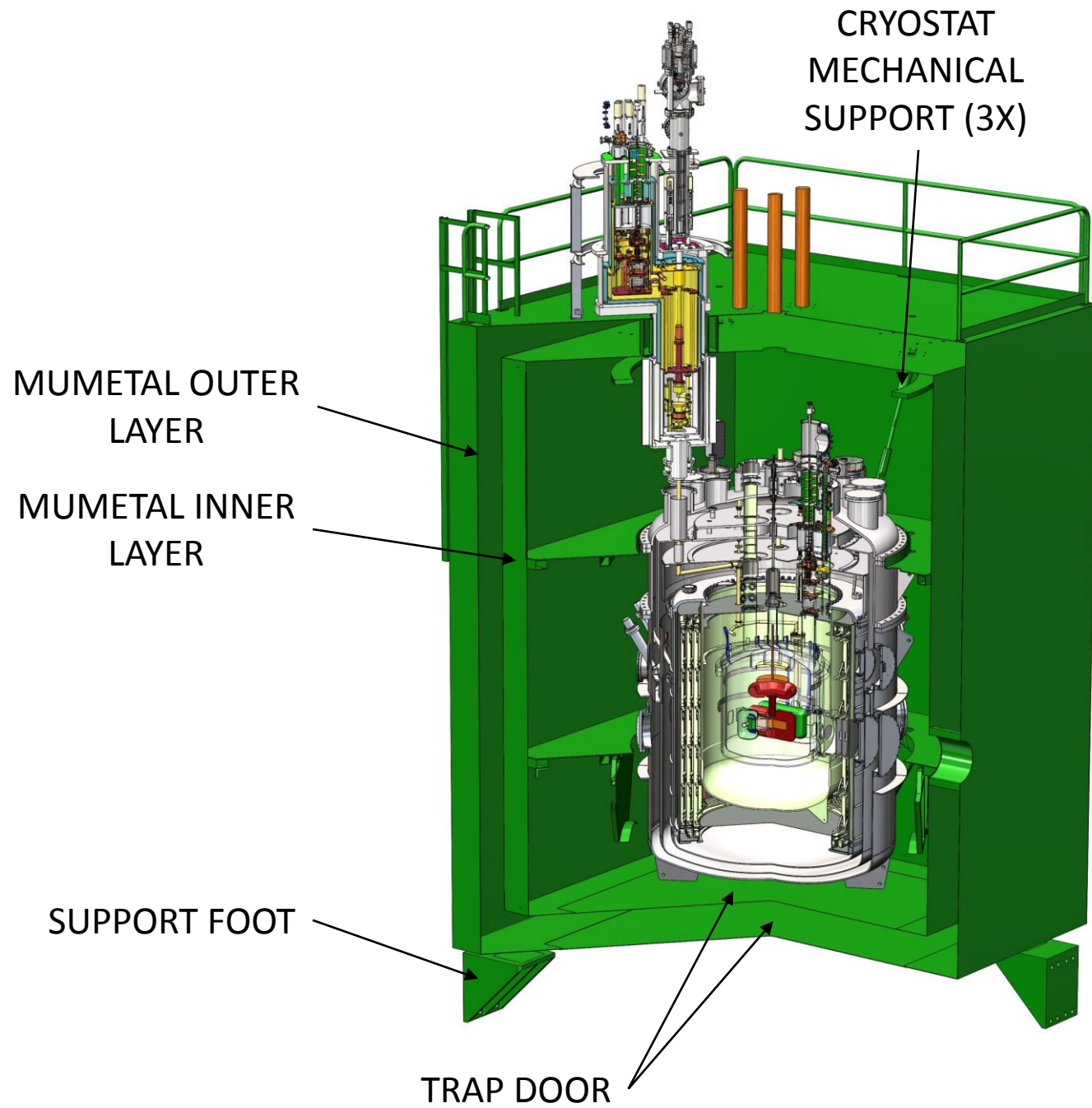


Credit: Brad Filippone, and collaborators, a paper submitted soon to JINST:
A New Apparatus for a Cryogenic Measurement of the Neutron Electric Dipole Moment

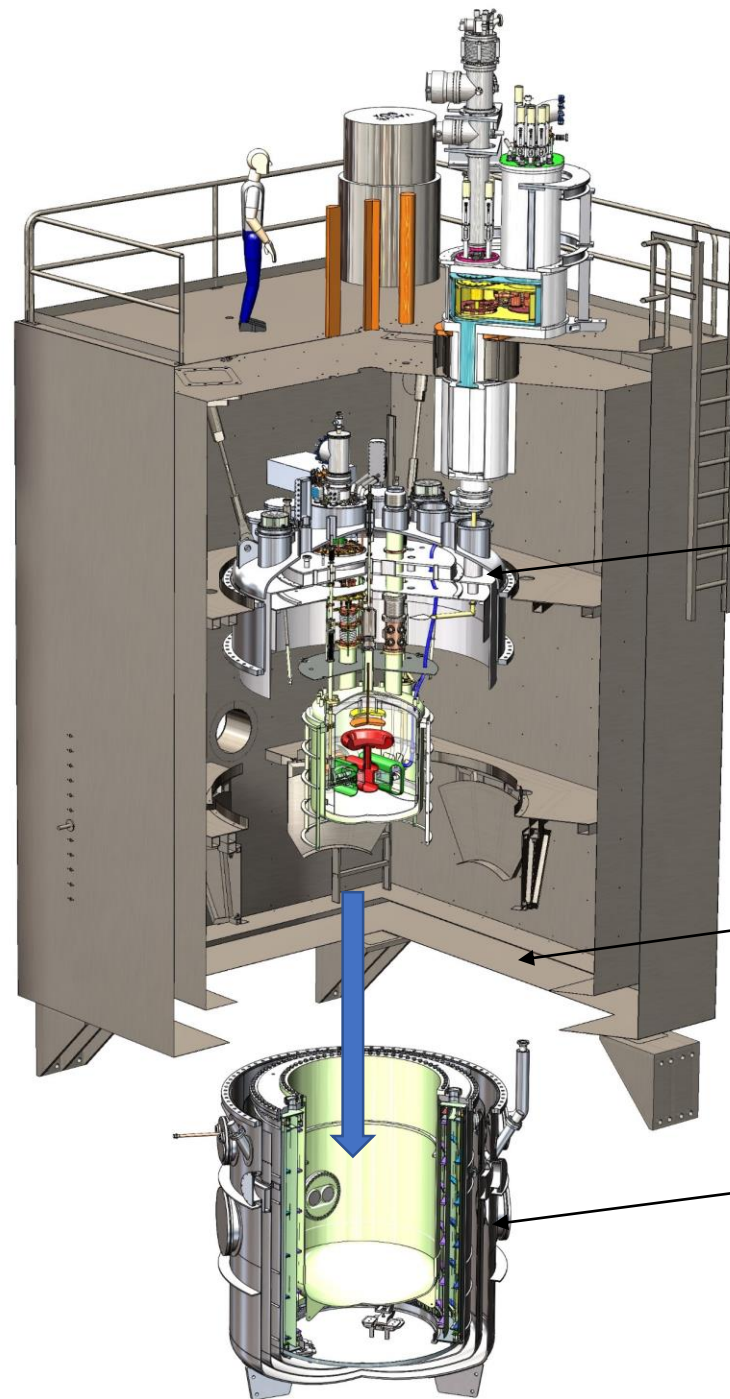
Apparatus Summary

- Magnetic fields
- Helium Transport
- Neutron Transport
- Central Detection
- Systematics
- PULSTAR Systematic Study apparatus





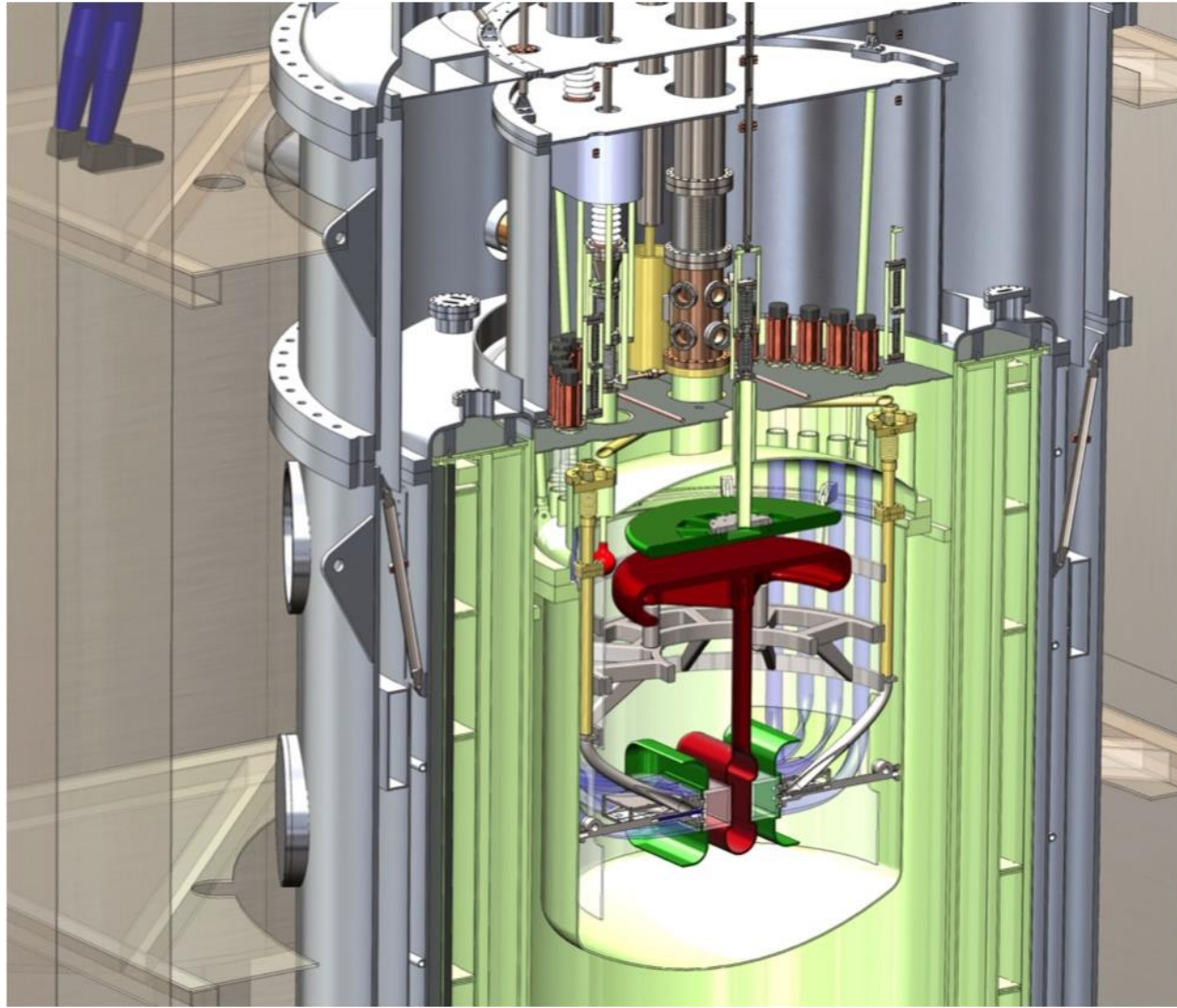
OVERALL APPARATUS MAGNET EXTRACTED



CDS MODULE
IN PLACE

SHIELD ROOM
TRAP DOOR OPENING

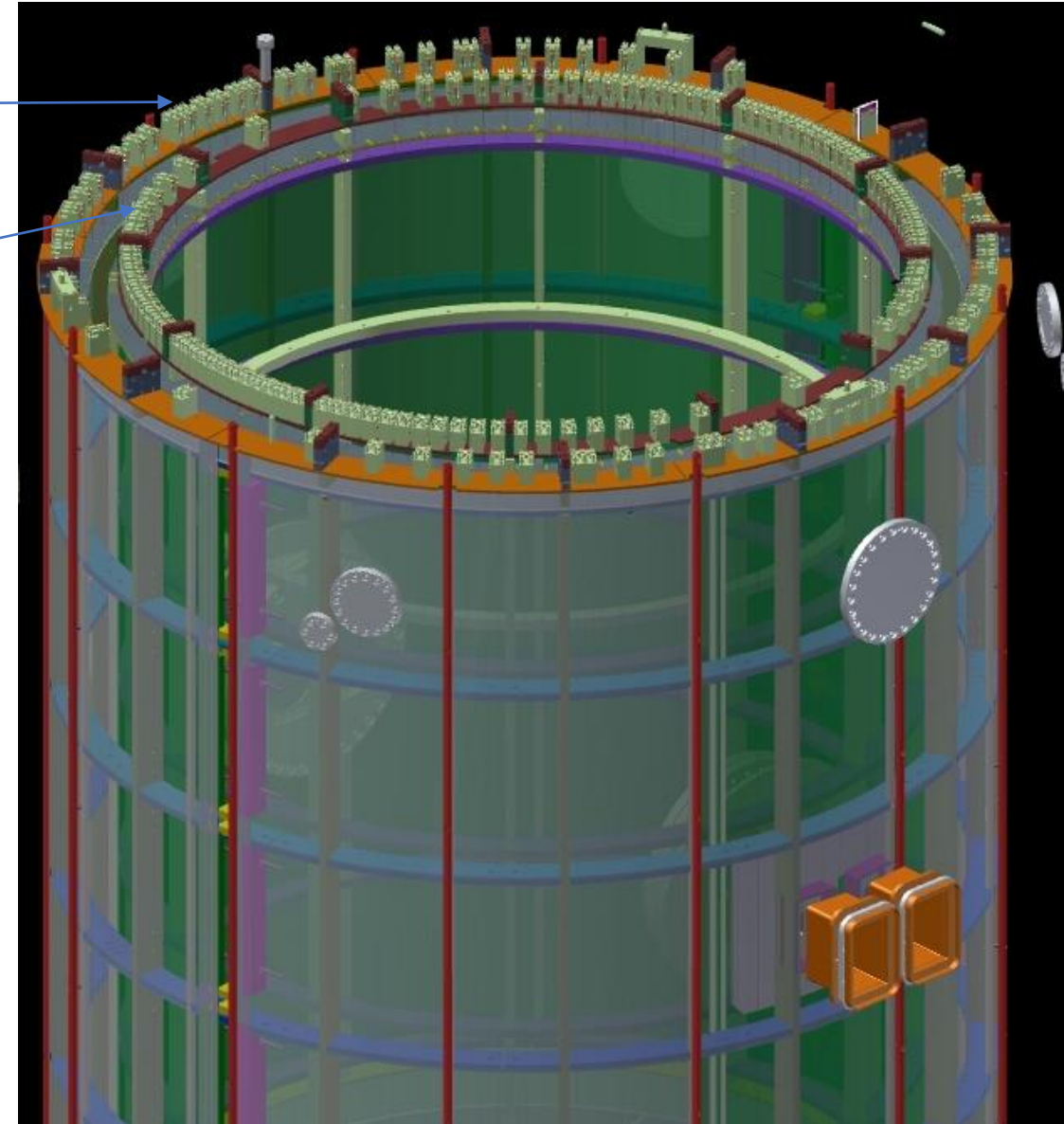
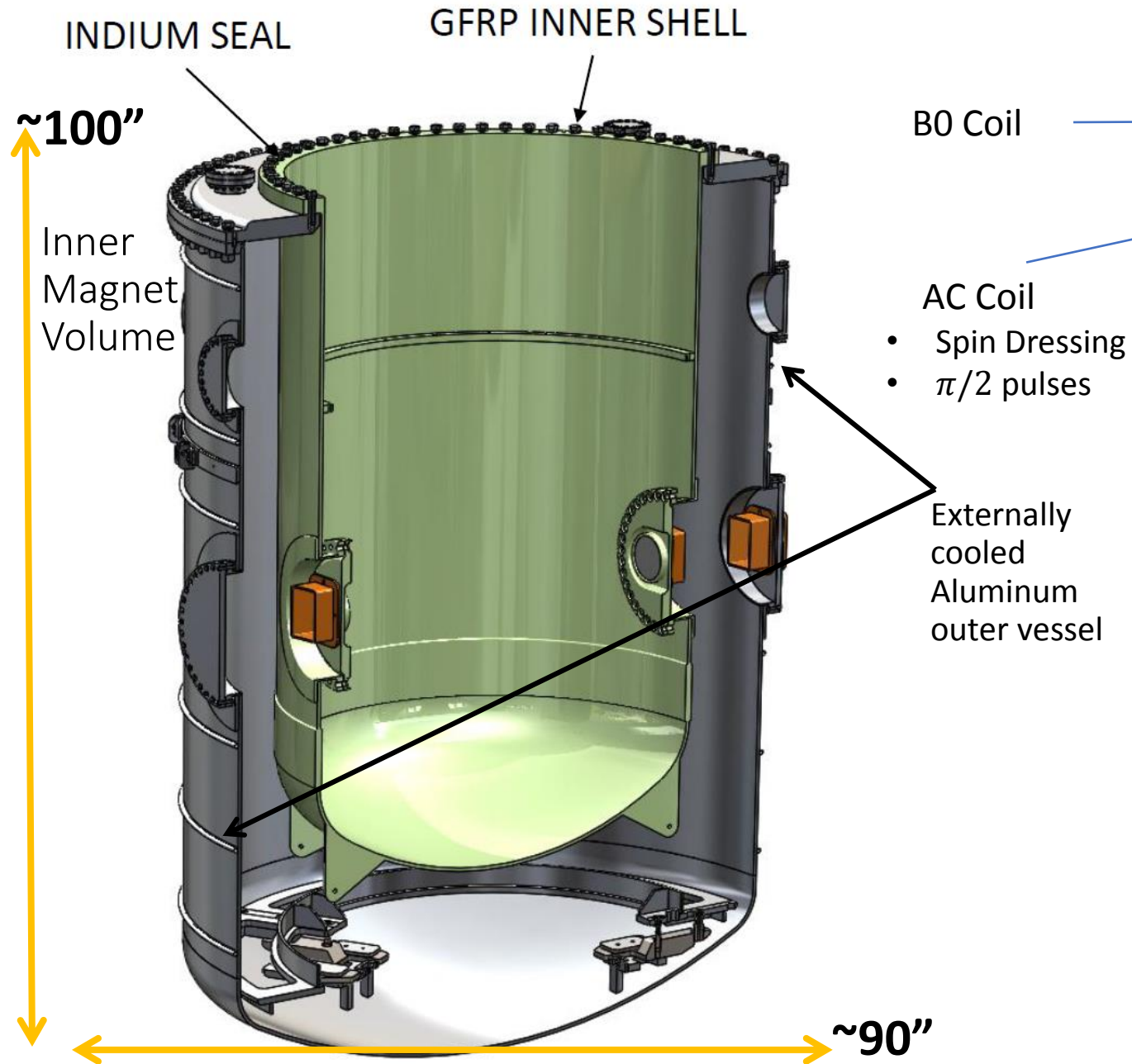
MAGNET MODULE
LOWERED



Commissioning Cryovessel and Outer LN Shield



Magnetic Fields



Field Monitoring system

Field Reconstruction via Scalar potential fitting

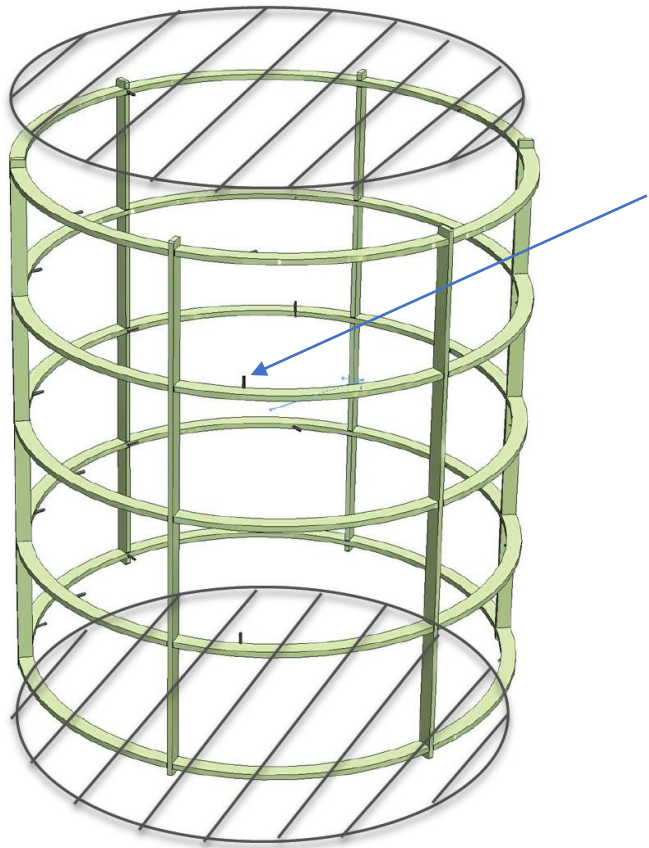
Simulated Sensitivity

$\sim 1 \times 10^{-4}$ mG/cm on Axis sensitivity

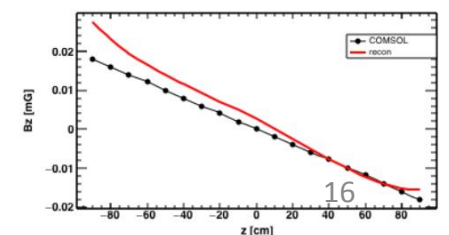
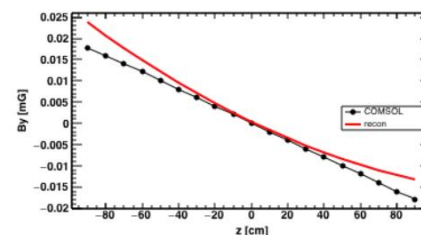
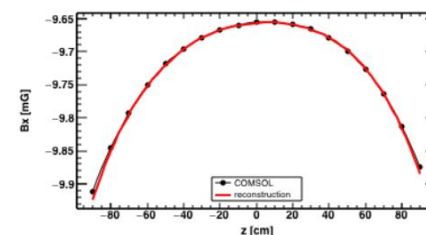
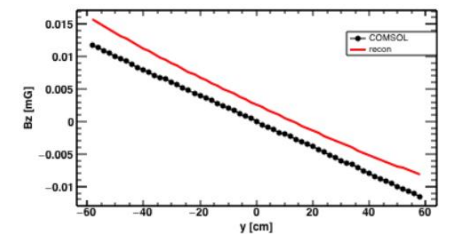
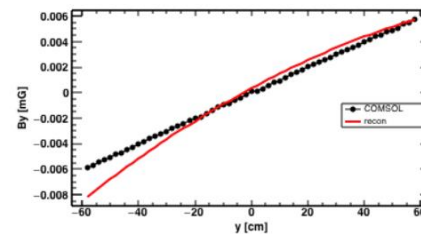
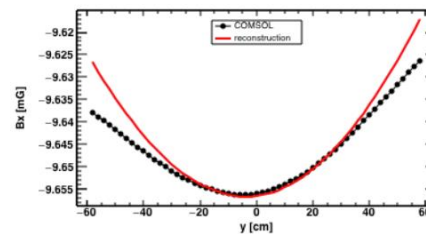
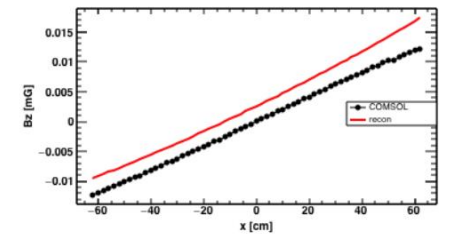
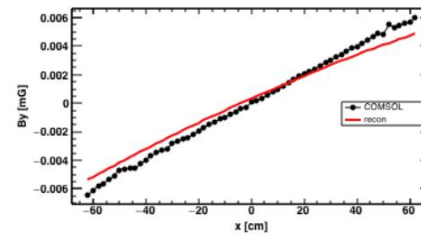
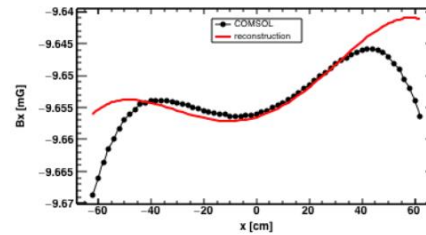
Can get more with 2 Radii of probes

This is sensitivity enough to shim a good T2

Gradient 3: $a = 0.0001$ mG/cm



Probes



Reconstruction Results of Real Data

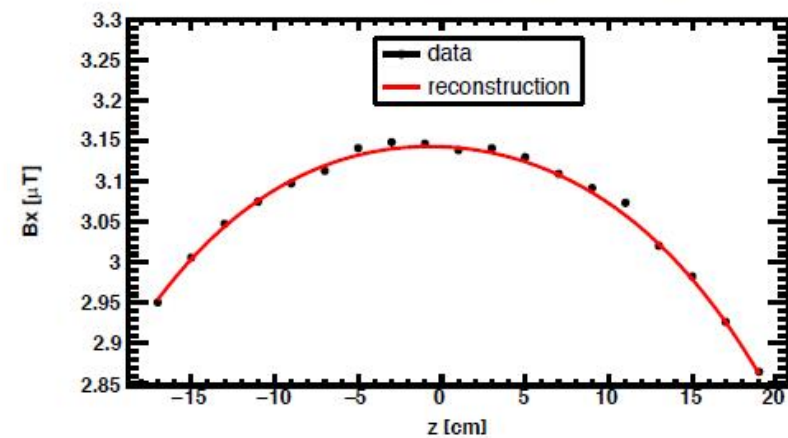
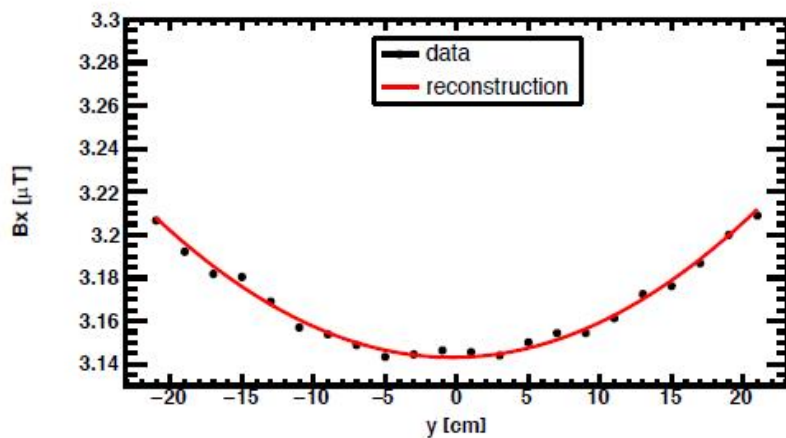
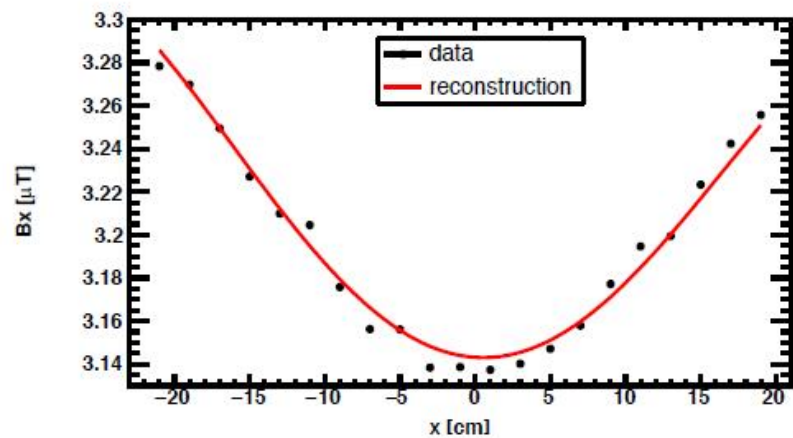
Field Cancellation and
Gradient Coils

B0 coil

Bartington
Triple Axis Probe



Reconstruction with 39 BV



B0 Coil Optimization Chris Swank

- Minimization of conditional density weighted field Fourier coefficients

$$\frac{1}{T_2} \propto S_B(0) = \sum_{l_x, l_y, l_z = -\infty}^{\infty} \underbrace{B_0(l_x, l_y, l_z) B(l_x, l_y, l_z)}_{\text{Particle Independent}} \underbrace{p\left(\left[\frac{l_x \pi}{L_x}, \frac{l_y \pi}{L_y}, \frac{l_z \pi}{L_z}\right], \omega\right)}_{\text{Particle Dependent}}$$

$d\omega \propto \omega \text{Im}(S_B) + \langle \mathbf{B}_x \cdot \mathbf{x} \rangle$

Thus, minimize

$$B(l_x, l_y, l_z) = \int_{-L}^L B(\mathbf{x}) \exp\left(-\frac{i\pi \mathbf{l} \cdot \mathbf{x}}{L_i}\right) d\mathbf{x}$$

³He Diffusion limit

$$p(q, \omega) = 2 \text{Re} \left(\frac{1}{\frac{kT}{m} q^2 \tau_c + i\omega} \right)$$

neutrons $\sum_{l_x, l_y, l_z = -\infty}^{\infty} \frac{B_0(l_x, l_y, l_z) B(l_x, l_y, l_z)}{(l_x^2 + l_y^2 + l_z^2)^{1/2}}$

Neutrons

(approximate as ballistic),

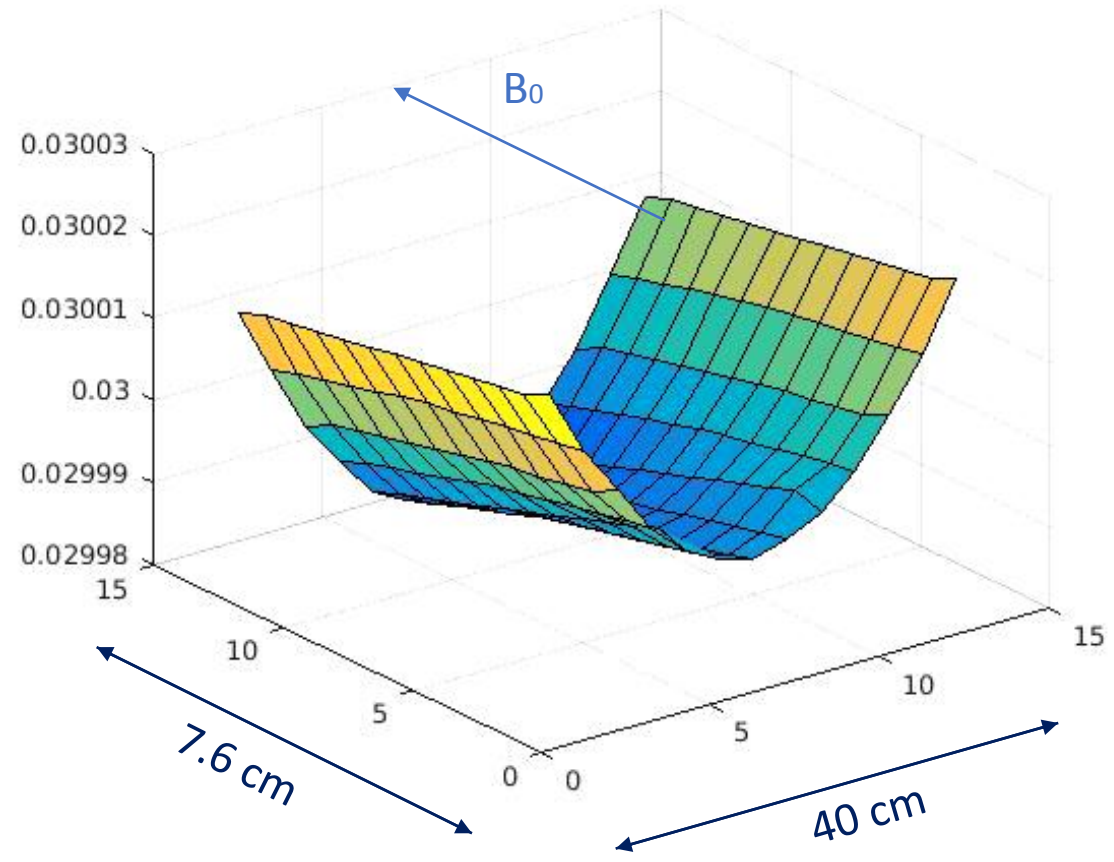
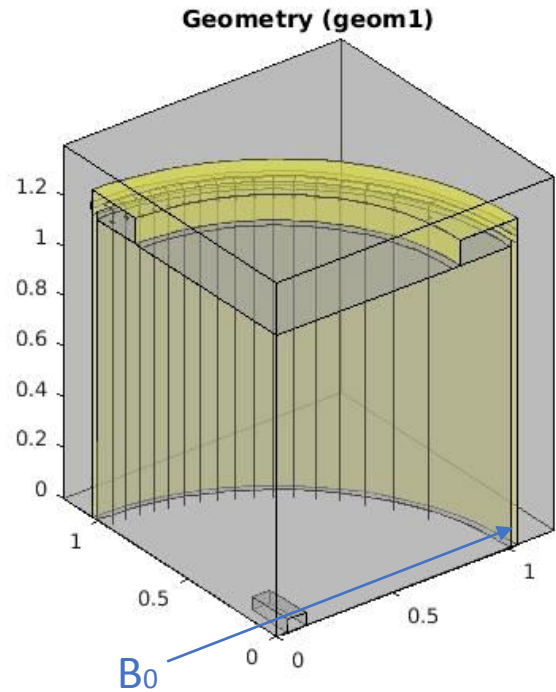
³He $\sum_{l_x, l_y, l_z = -\infty}^{\infty} \frac{B_0(l_x, l_y, l_z) B(l_x, l_y, l_z)}{l_x^2 + l_y^2 + l_z^2}$

$$p(q, \omega) \propto \frac{1}{|q|}$$

B₀ Field is not parallel to gravity!

Computationally fast due to modern FFT algorithms.

Optimization Example

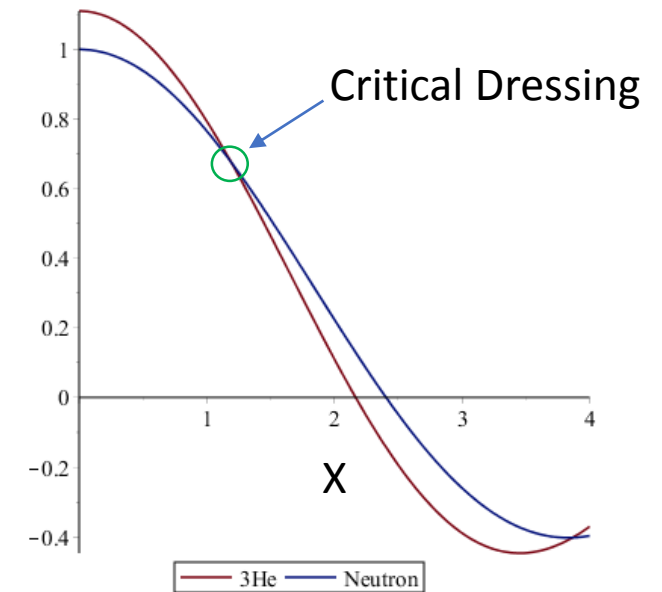


Spin Dressing and Critical Dressing

- Spin dressing can be applied so that.

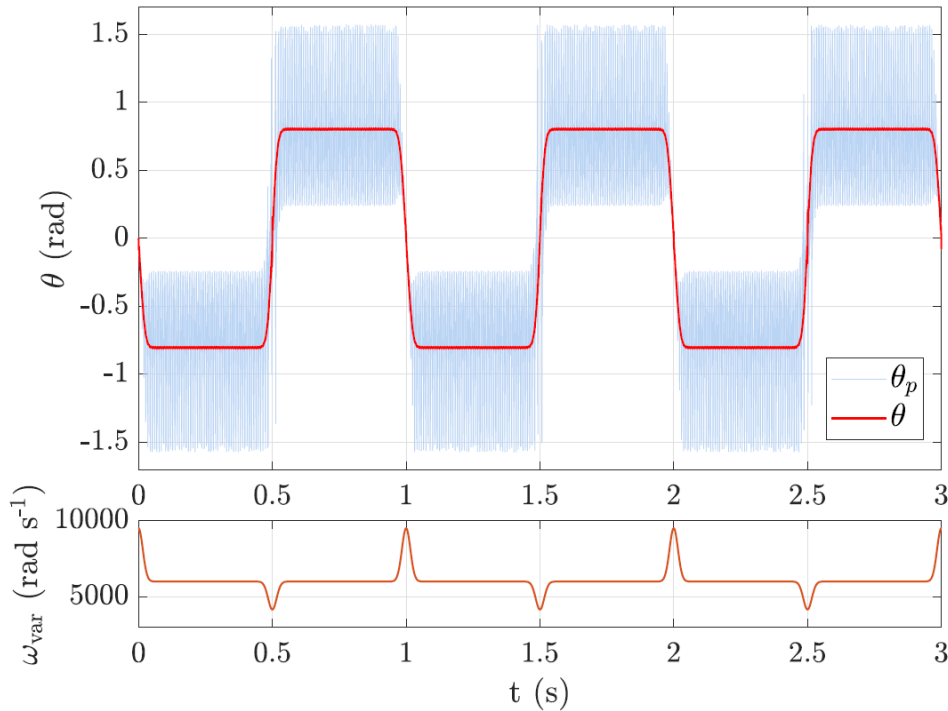
$$J_0(X_c) = \alpha J_0(\alpha X_c) \quad X_s = \frac{\gamma_s B_{\text{rf}}}{\omega_{\text{rf}}}$$

- For neutrons and ^3He $\alpha=1.11$. And X_c is the critical dressing parameter,
- Dressed with this parameter the two spin species will have the same effective precession.
- With this technique we can set $\langle \sigma_n \cdot \sigma_3 \rangle$ at the optimum and leave it
- Factor 2 improved sensitivity

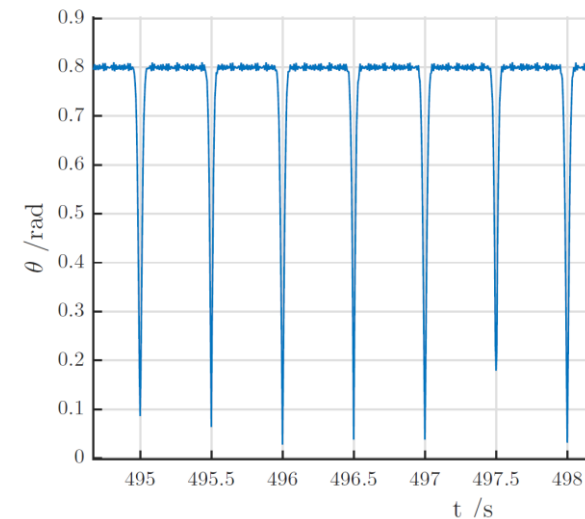


Modulated Critical Dressing.

- Systematic effects can be mitigated by modulation
 - Maintain maximum sensitivity by modulating to maximum sensitivity phase.



$$\langle \sigma_n \cdot \sigma_3 \rangle = \frac{1}{2} [1 + J_0(x_n - x_3)] \cos(\omega'_n t - \omega'_3 t - \phi_0) + \frac{1}{2} [1 - J_0(x_n - x_3)] \cos(\omega'_n t + \omega'_3 t + \phi_0)$$



Fast oscillations can be used for diagnostics

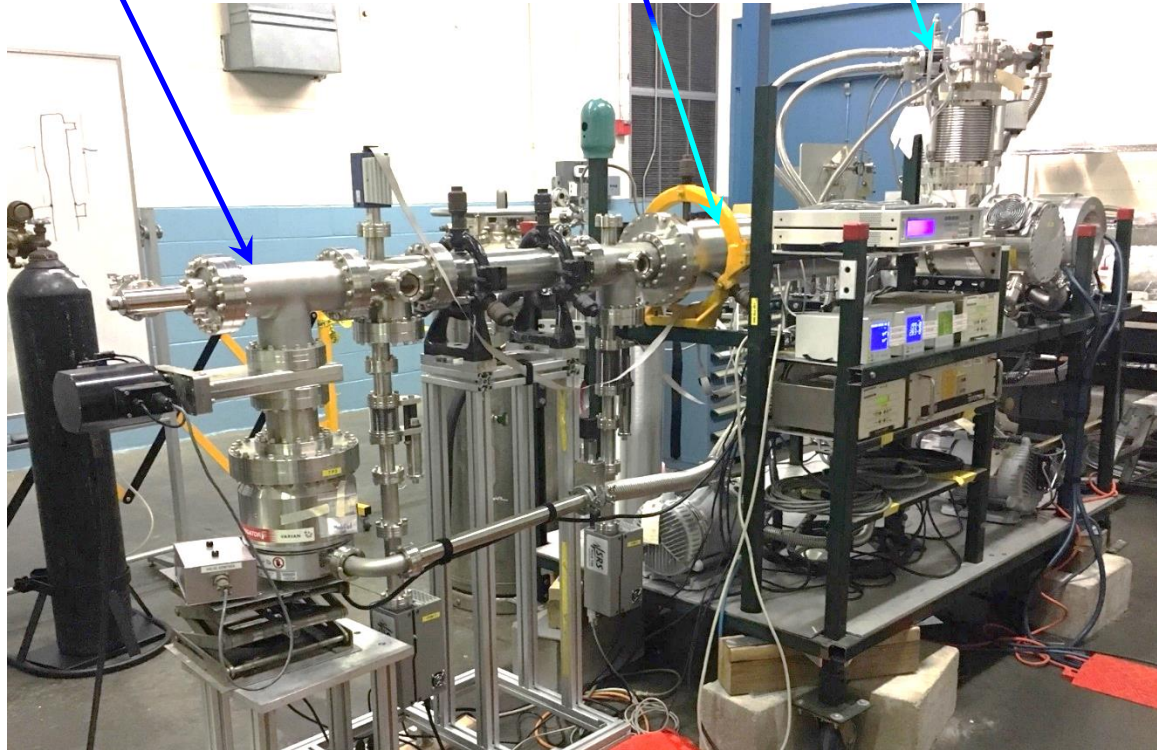
Polarized ^3He Source: Atomic Beam Source (ABS)

ABS installed in the test apparatus

Flux Divergence test chamber (not connected)

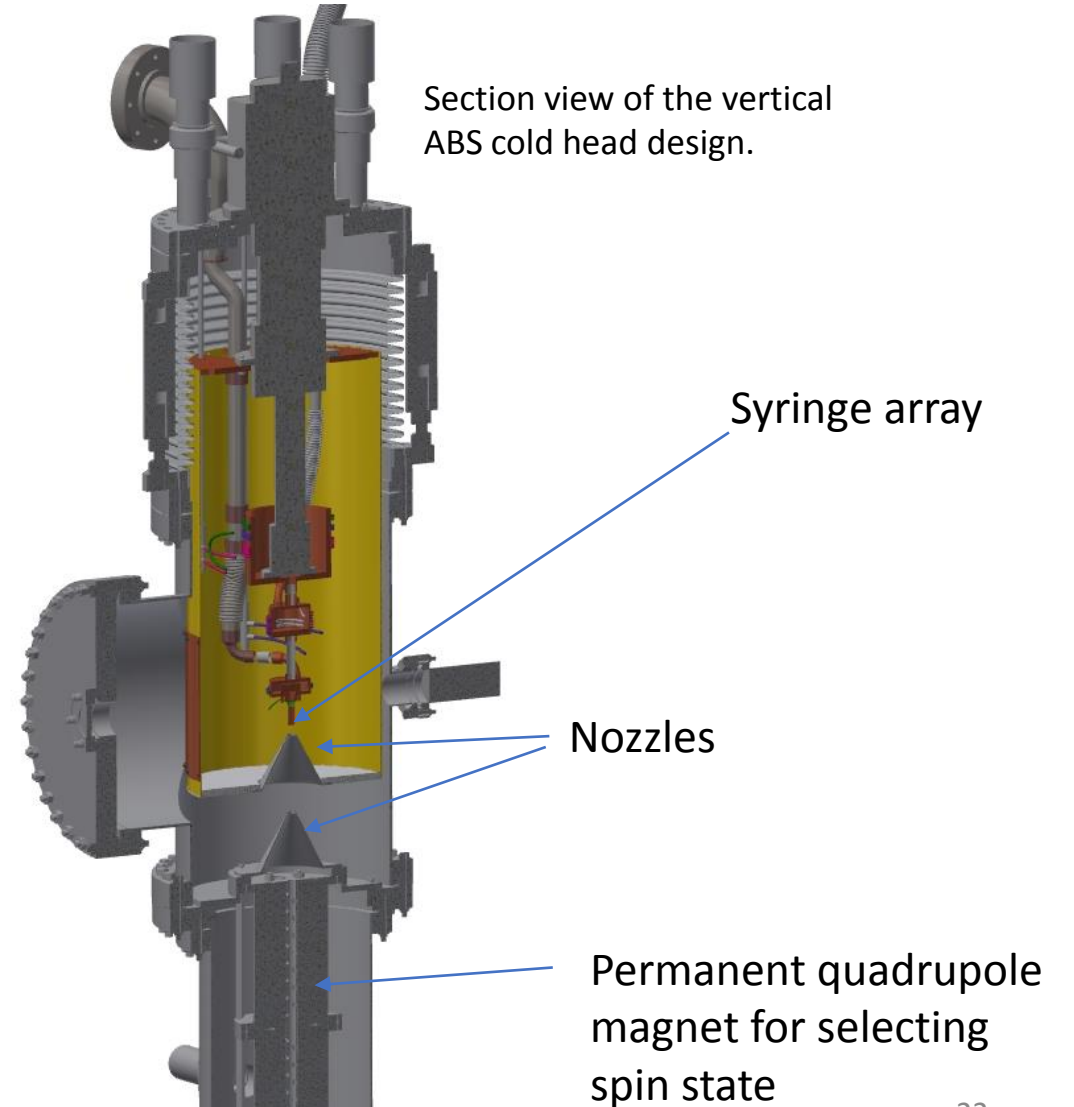
Polarizer beamline

Cold head



The atomic beam source setup at MIT/Bates

Section view of the vertical ABS cold head design.



Heat Flush into the measurement cell

- The heat flush can be modeled in different ways.

- ^3He transport determined from convection diffusion

$$\frac{\partial x_3}{\partial t} + \vec{v}_{ph} \cdot \nabla x_3 = \nabla \cdot (D_{3,ph} \nabla x_3)$$

- 1D, phonon velocity determined from heat transport equation

$$\vec{Q} = TS_{ph} \vec{v}_{ph}$$

- 3D, phonon transport determined from Navier Stokes

- Required for best accuracy in spin tracking CHANGE TO v_{ph}

$$\rho_{ph} \left(\frac{\partial v_{ph}}{\partial t} + v_{ph} \cdot \nabla v_{ph} \right) = -\nabla p_{ph} + \eta_{ph} \nabla^2 v_{ph}$$

First heat flush is solved in COMSOL via Navier-Stokes.

$$\rho_n \left(\frac{\partial \mathbf{v}_n}{\partial t} + \mathbf{v}_n \cdot \nabla \mathbf{v}_n \right) = -\nabla p_n + \eta_n \nabla^2 \mathbf{v}_n$$

Temperature derived
from pressure

$$\begin{aligned} dp &= SdT \\ S_n(T) &= \frac{2\pi^2 k_B^4}{45 \hbar v_T^3} T^3 \\ p(T) &= \frac{2\pi^2 k_B^4}{180 \hbar v_T^3} T^4, \end{aligned}$$

Viscosity and density
are given by

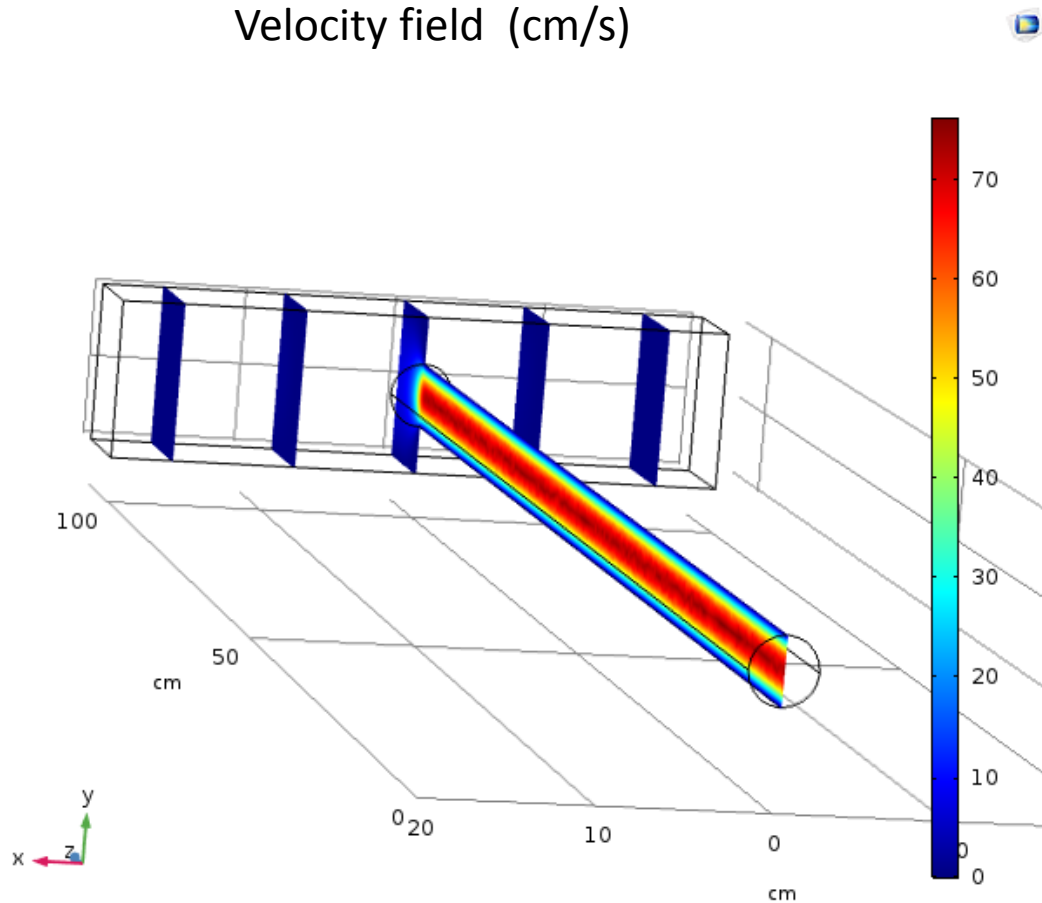
$$\begin{aligned} \eta &= \rho_n \frac{\lambda u}{3} \\ \rho_n &= \frac{2\pi^2 k_B^4}{45 \hbar^3 u^5} T^4 \\ u &= 24000 \frac{\text{cm}}{\text{s}} \\ \lambda &= \left(1.28 \times 10^{-5} T^{-9} + 3.80 \times 10^{-3} T^{-4} \right) [\text{cm}]. \end{aligned}$$

For those interested (cgs):
 $p=2492.2T^4$ (dyn/cm²),
 $\rho_n=1.7305e-5T^4$ (g/cc)

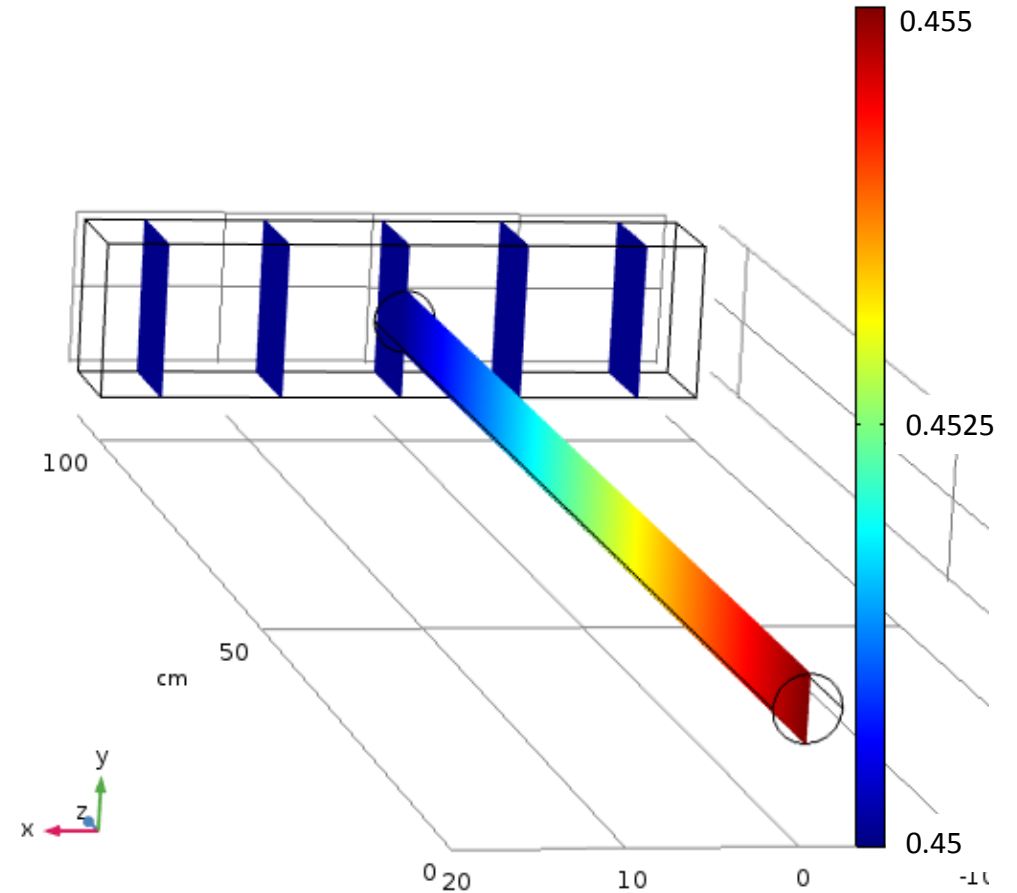
Visualization of COMSOL Navier Stokes Solution.

This example is steady state, time can be included (4D quad-cubic spline, more time to solve)

Velocity field (cm/s)



Temperature (K)



Rectangular mesh data file is imported into c++,
tri-cubic spline built for data interpolation.

Building 2 Non-magnetic Dilution Refrigerators

Chris Swank

Design Goal:

80 mW at 300 mK

Still

Mixing Chamber



Currently Stainless Steel heat exchangers (a little magnetic)

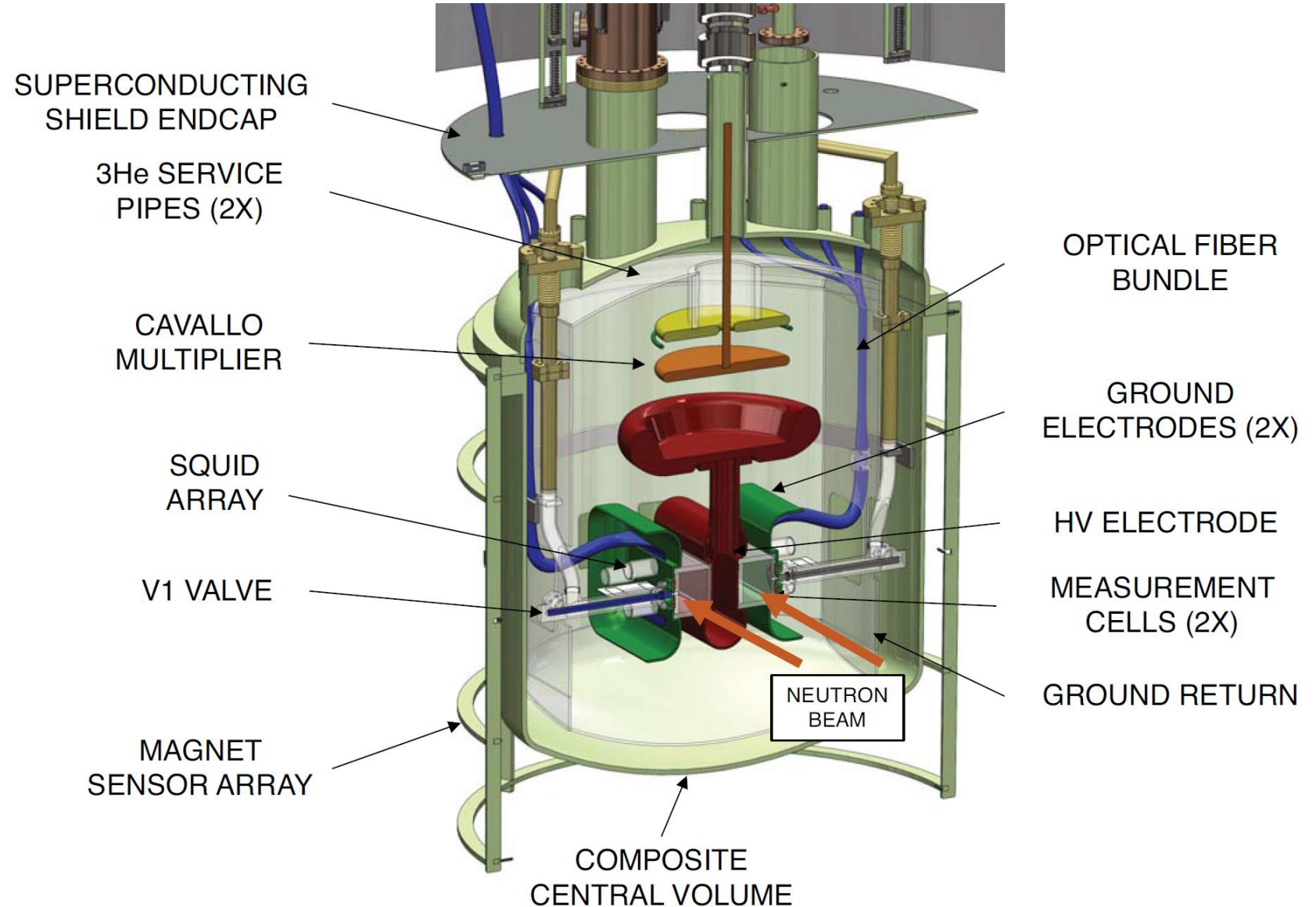
2nd Fridge will be German Sivler (non Magnetic)

Credit: Weijun Yao

Central Detection System

Highlights

- 75 kV/cm Electric field
- Cavallo's Multiplier
- Squid Magnetometer
- 1600 L of super fluid helium
- Light collection



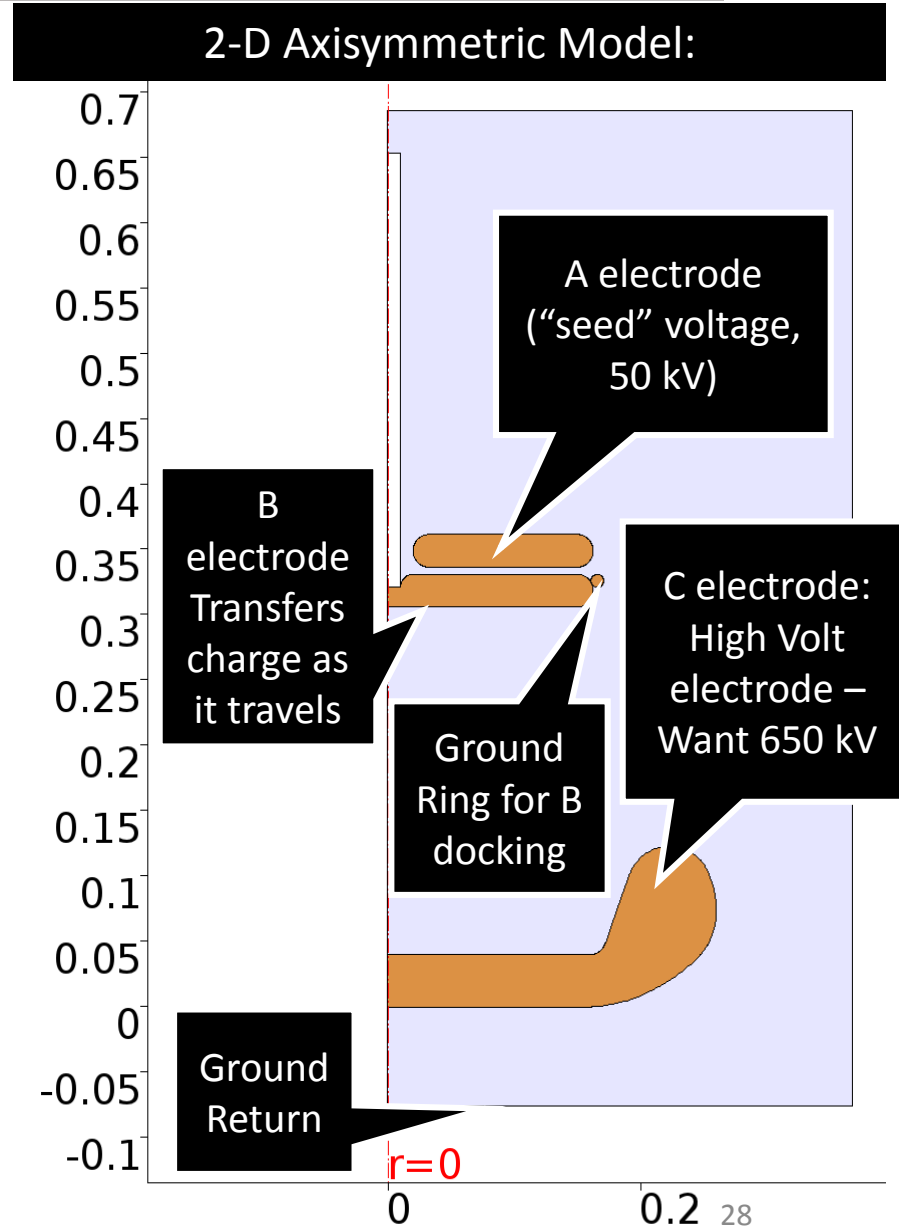
Cavallo Refresher: Marie Blatnik

Cavallo Electrode Simulation Constraints:

1. Maximize Output Voltage (at least 650 kV).
2. E fields $< \sim 100$ kV/cm.
3. Small input voltage V_A (50 kV).
4. Restricted Diameter ($\sim 30''$) with length to spare.

Cavallo Electrode Reality:

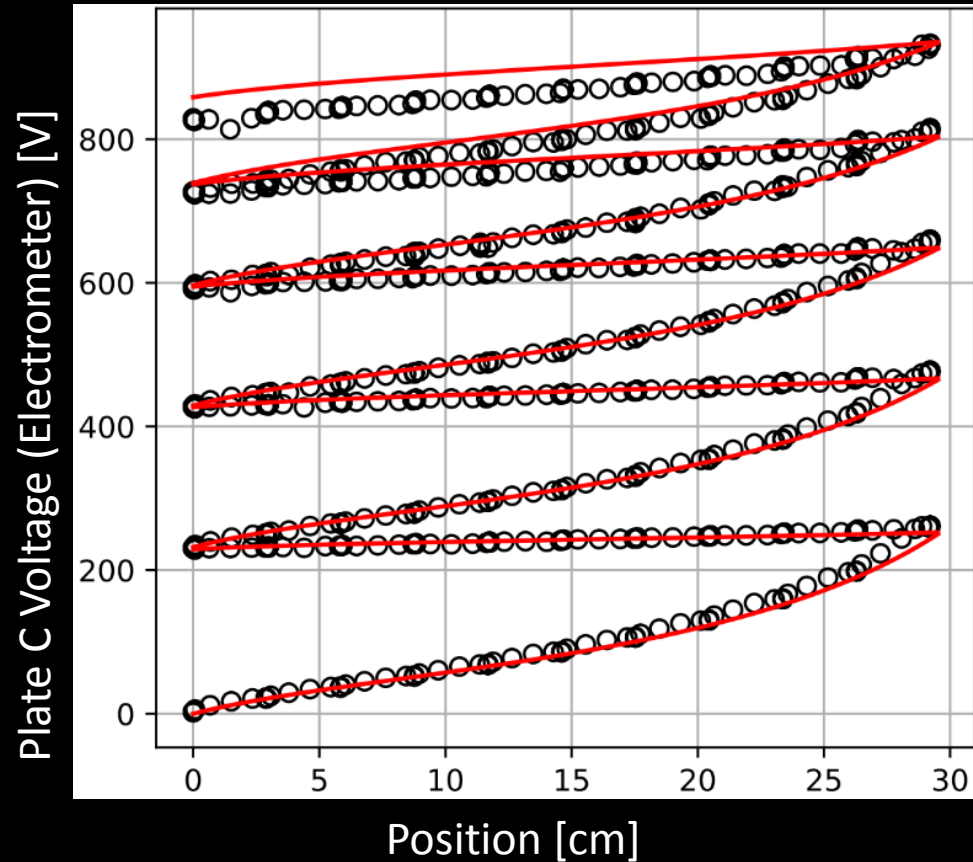
Endeavor to fabricate this design and test them in the Caltech dewar.



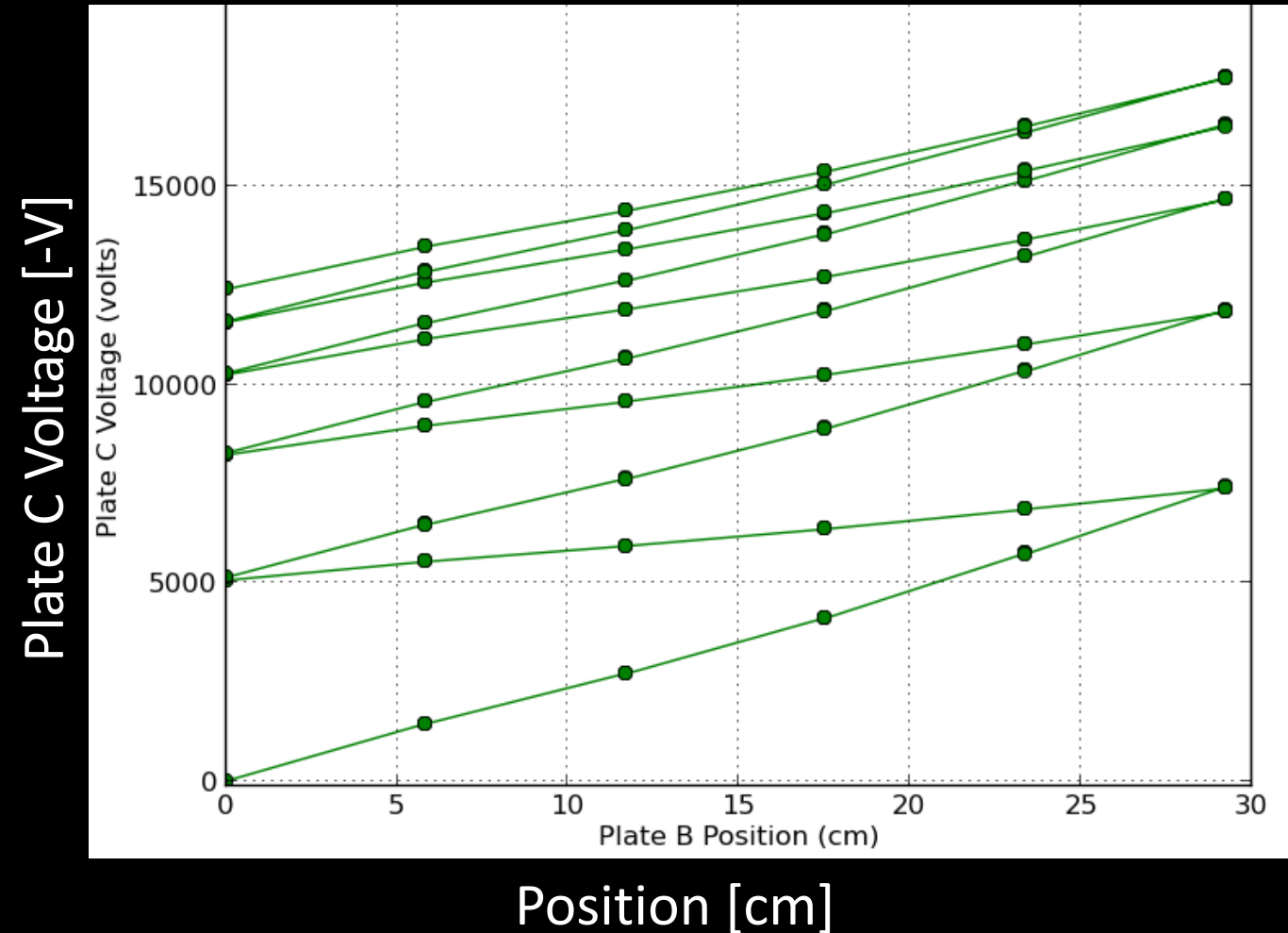
ROOM TEMPERATURE APPARATUS

Marie Blatnik

C Electrode Voltage vs B Position



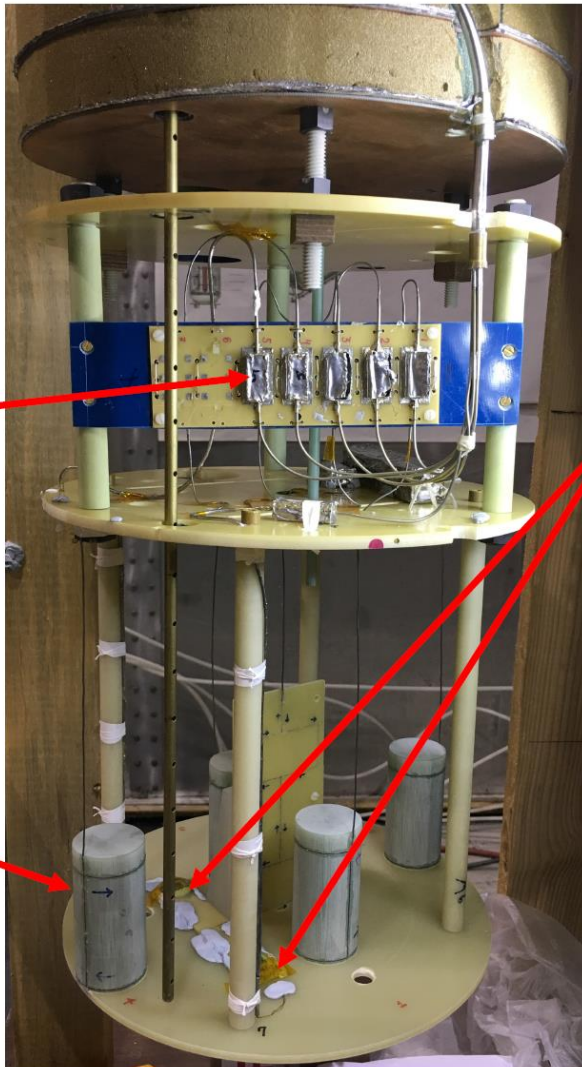
C Electrode Voltage vs B Position



We can use the PD410 from PI to wiggle cryogenically

SQUID System

SQUIDs
Multichannel
Prototype



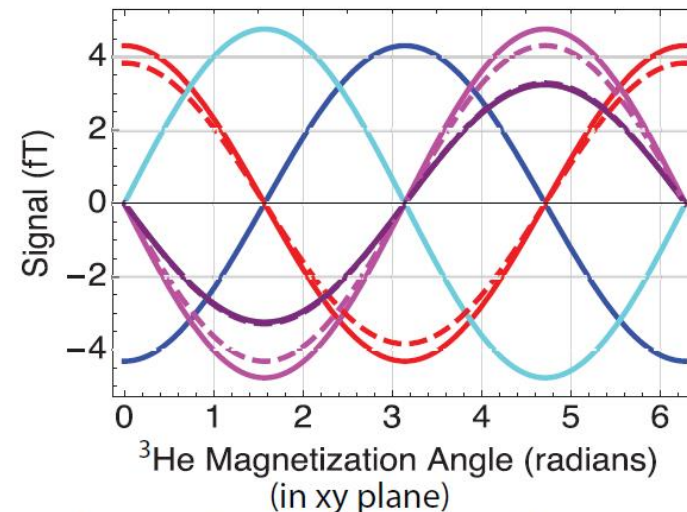
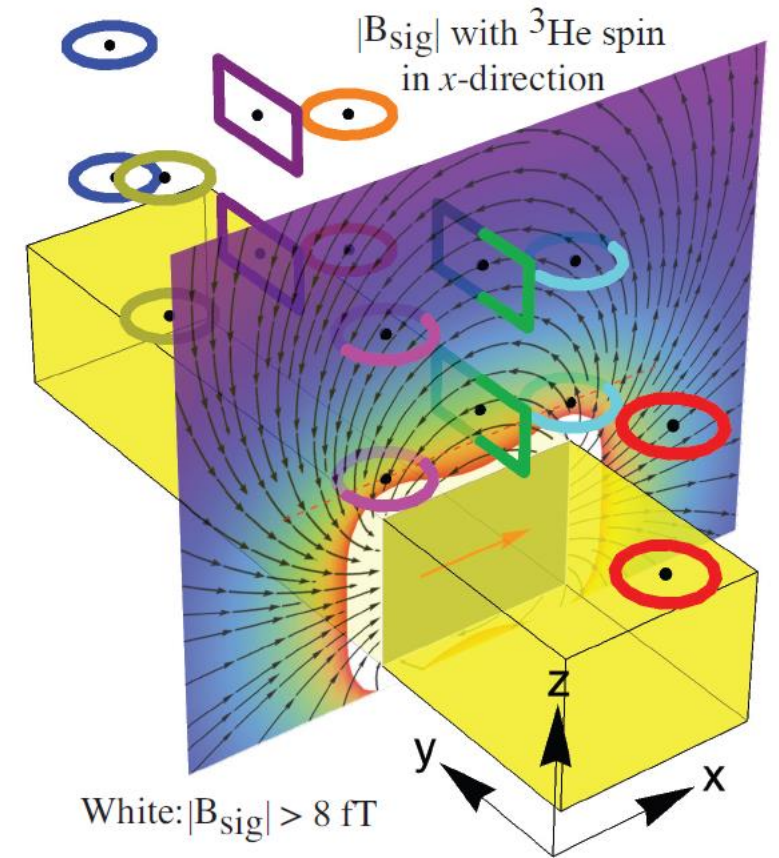
SQUIDs in
Pb boxes

Axial pickup
loop

Distance between inside
bottom of dewar (4 K)
and outside (RT): 24 mm

Integrated
magnetometers from
Supracon/Jena

“AC defluxing” coils will be
installed on the integrated
magnetometer chips for
this test. Matlashov et al.,
IEEE TAS, **27**, no. 4, June
2017.



Squid System
Expected SNR \approx 6

PULSTAR Systematic Apparatus

Relatively agile apparatus compared to SNS nEDM (short turn around time)

Perform Systematic Studies

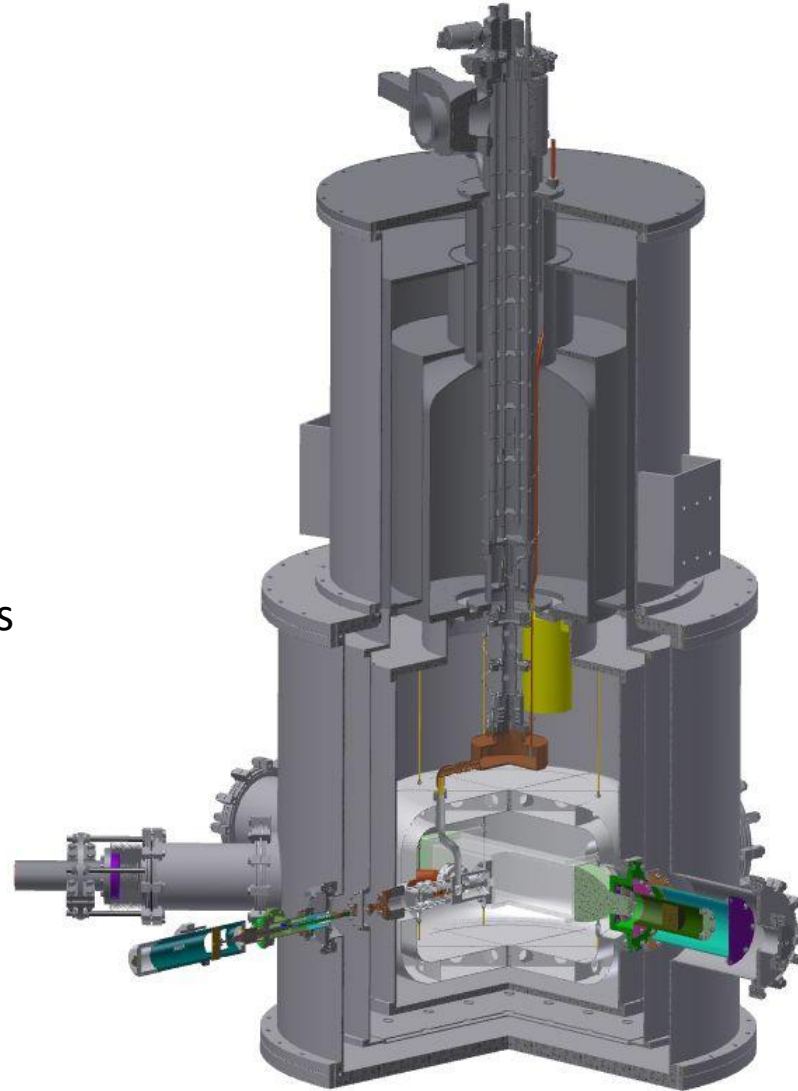
- Correlation function measurements
- Predictions of Geometric Frequency shift

NMR/Spin Dressing pulse optimization

- $\pi/2$ pulses, critical dressing parameters

Cell Storage Studies

- Determine cell quality prior to implementation into SNS nEDM apparatus.
- Estimated to reduce time to data taking by more than 1 year.



Commissioning

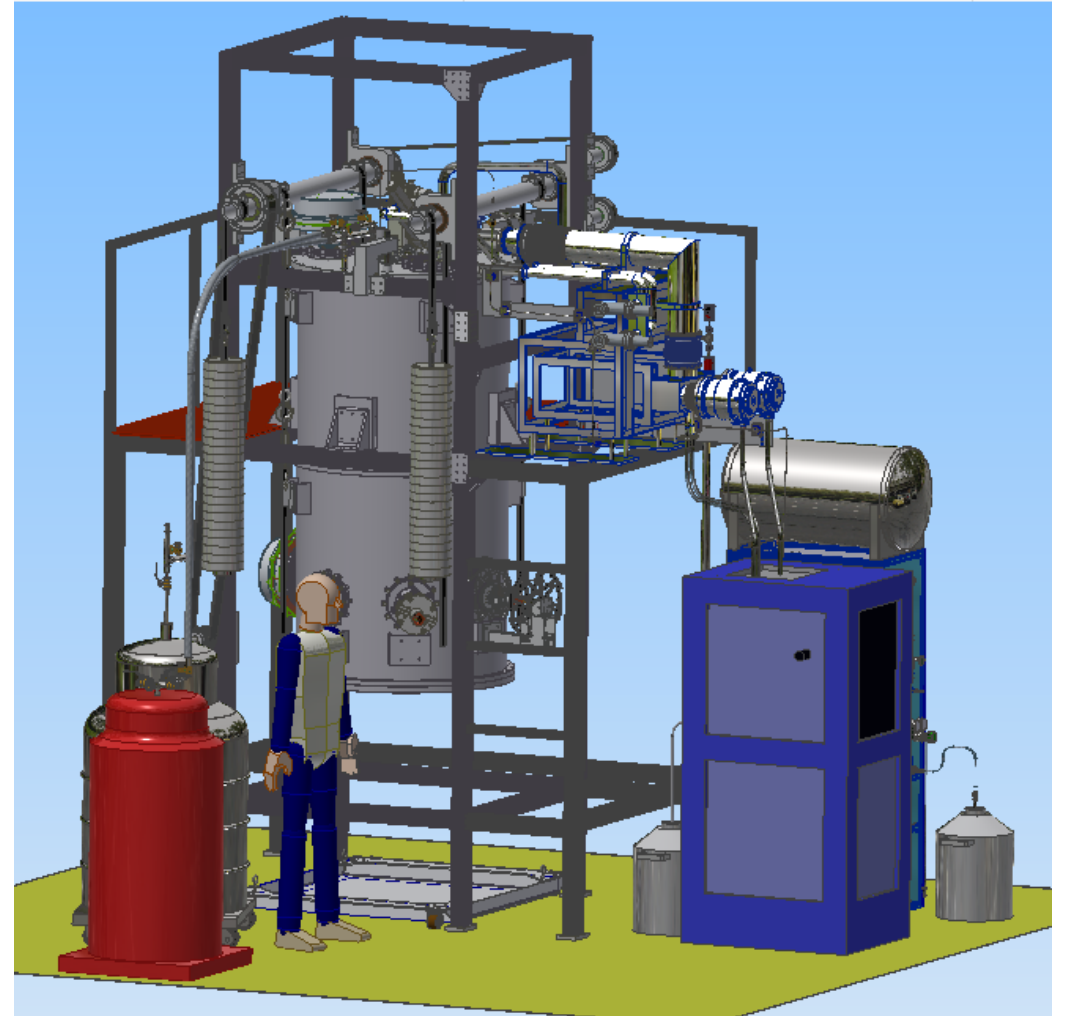


Solid Deuterium Source



Overview

- Test bed for SNS nEDM
- Contains many similar systems to nEDM
- Is being constructed at Triangle Universities Nuclear Laboratory (TUNL) in Durham NC on Duke campus
- Once commissioning is complete, a study of the Correlation Function (Barry Shift) will be conducted with ^3He
- The cryostat will then be moved to the PULSTAR reactor on NC State campus, where UCN will be placed inside the measurement cell with polarized ^3He



Comparing SOS to nEDM

Similarities

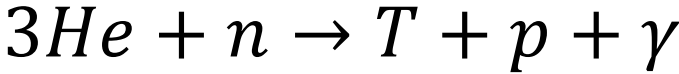
- Experiments conducted at 0.4K
- Nuclear Magnetic Resonance (NMR)
- Superfluid Helium
- Polarized ^3He
- Ultra-cold Neutrons (UCN)
- LHe scintillation
- Light collection with Silicon Photomultipliers (SiPM)
- Superconducting QUantum Interference Devices (SQUIDs)
- Critical spin dressing
- Same size measurement cell

Differences

- No electric field
- Meta-stability optical pumping for polarized ^3He (SOS) vs Atomic beam source (nEDM)
- SQUIDs in vacuum (SOS) vs LHe (nEDM)
- Single measurement cell (SOS) vs Two measurement cells (nEDM)
- 1 week to cool (SOS) vs 6 months to cool (nEDM)

SOS Operation

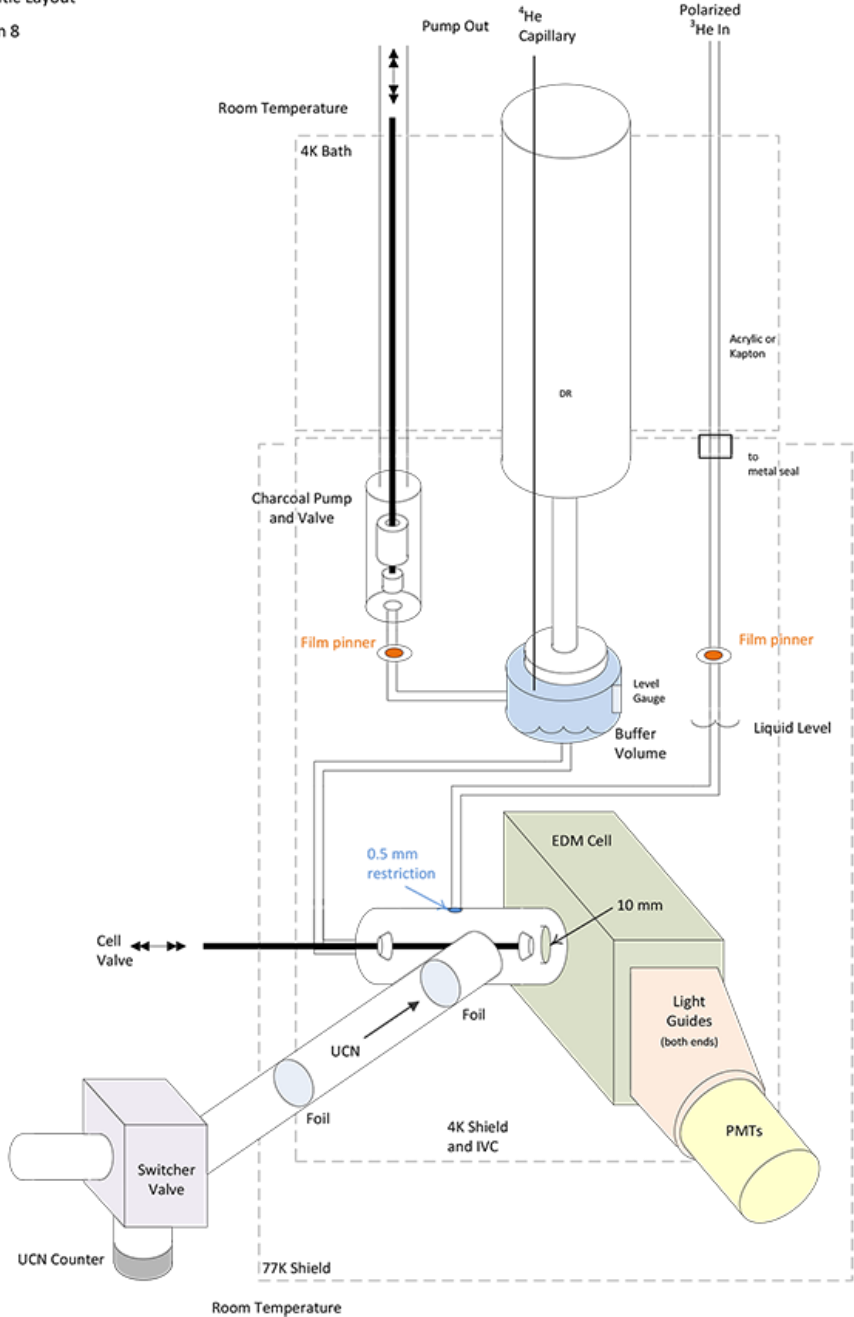
- Measurement cell is filled with 4He at 0.4K
- UCN are delivered from PULSTAR reactor
- Polarized 3He and UCN are placed in measurement cell

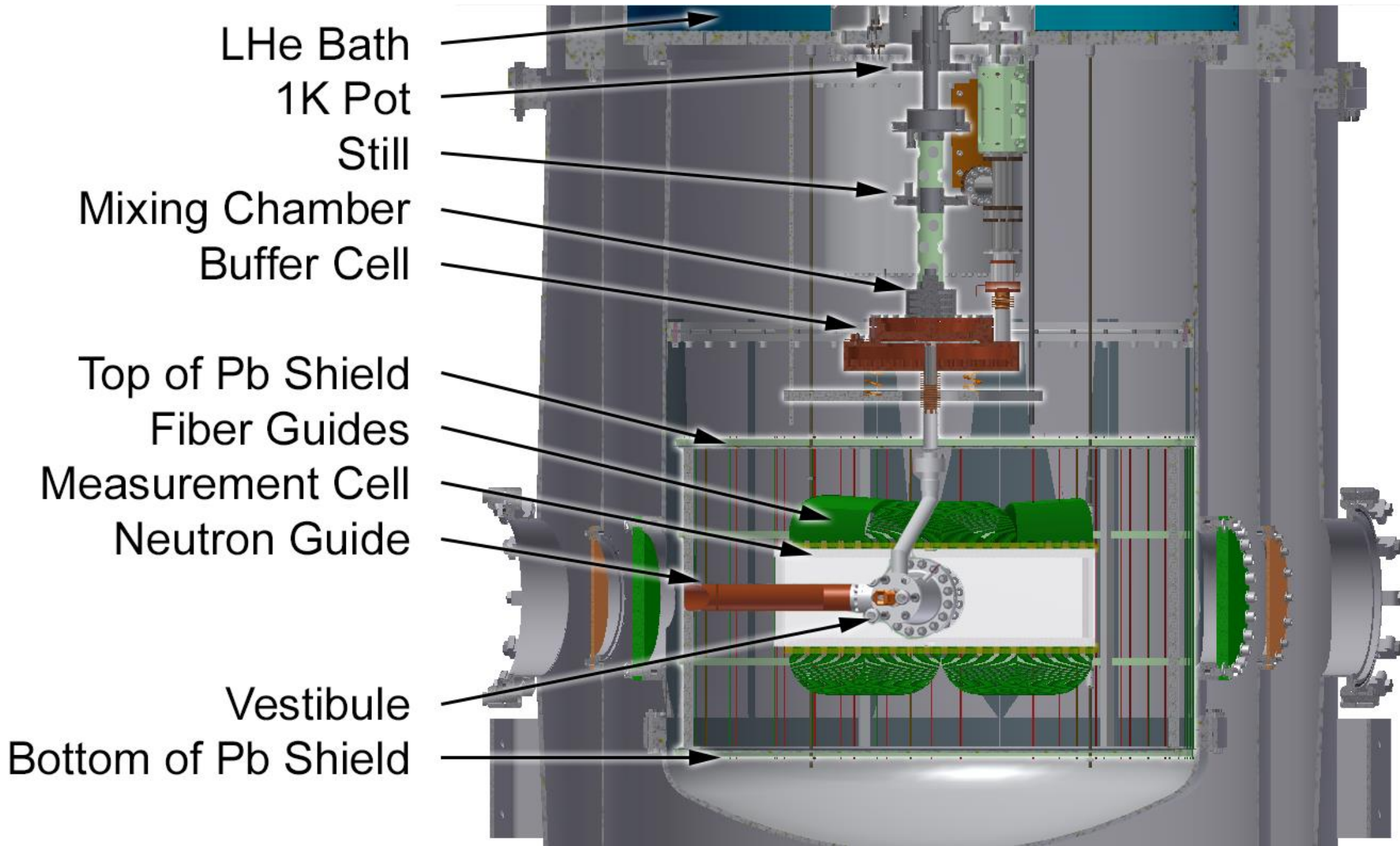


- This is a spin dependent interaction with rate

$$S(t) = \frac{\rho_{UCN} V}{\tau_{3\text{He}}} (1 - P n P_{3\text{He}} \cos \theta_{n, 3\text{He}}(t))$$

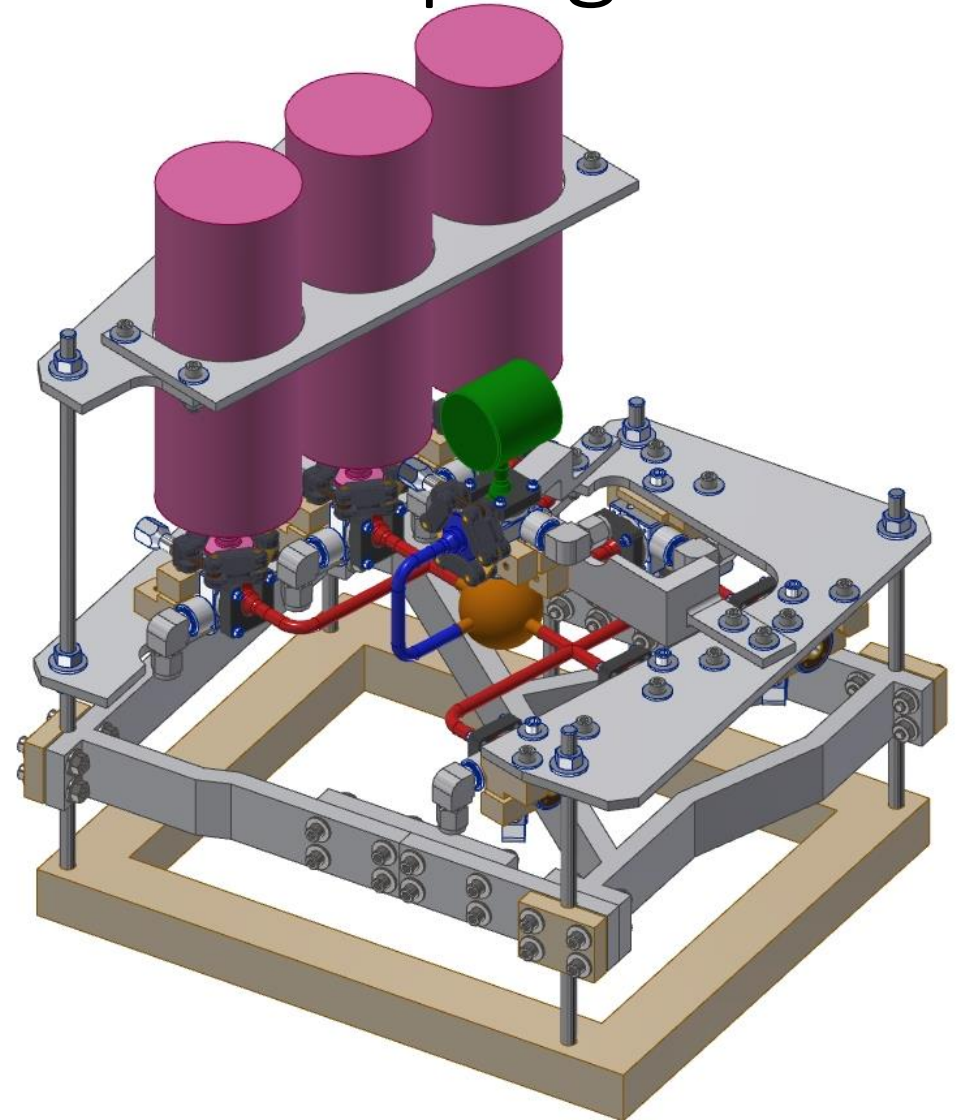
- Orientation of 3He is monitored using SQUIDS.
- Rate of interaction is monitored through light collection.





MEOP - Meta-stability Optical Pumping

- Polarizes ^3He at 1 mbar using electric RF, magnetic field, and laser
- Has three 1 liter dilution volumes for dilution down to desired concentration of $[\text{4He}:\text{3He}] = 10^{-9}$
- Polarized ^3He friendly valves - ILL design
- Once ^3He is polarized and rarified, ^4He will be added to increase the pressure (0.5 bar) before being transported to the measurement cell. This will overcome the LHe vapor pressure.



Thermalizing gas collisions

Scattering density

$$\rho(\mathbf{x}, t, \mathbf{v}) = \underbrace{f(\mathbf{x}, t, \mathbf{v})\alpha(\mathbf{v})\psi(t)}_{\text{Direct transport}} + \underbrace{\int d^3\mathbf{x}' dt' f(\mathbf{x} - \mathbf{x}', t - t', \mathbf{v})\psi(t - t') \int d^3\mathbf{v}' \beta(\mathbf{v}|\mathbf{v}') \rho(\mathbf{x}', t', \mathbf{v}')}_{\text{Previous scattering}}$$

Velocity change kernel

Direct transport

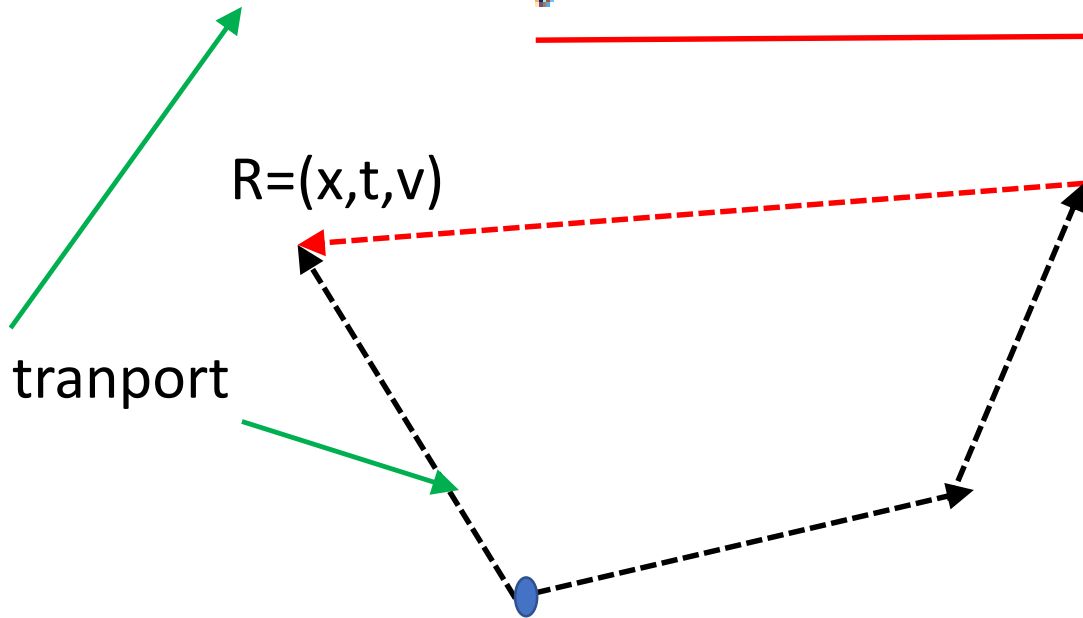
$R=(x,t,v)$

$R'=(x',t',v')$

R_0

$\psi(t)dt$

Probability of scattering between t and $t+dt$



$$\int d^3\mathbf{v}' \beta(\mathbf{v}|\mathbf{v}') \alpha(\mathbf{v}') = \alpha(\mathbf{v}),$$

Condition for thermal equilibrium

$$\Psi(t) = \frac{t}{\tau_c} = e^{-t/\tau_c}$$

$g(\mathbf{x}, t, \mathbf{v})$

$$\rho(\mathbf{x}, t, \mathbf{v}) = \alpha(\mathbf{v}) \boxed{f(\mathbf{x}, t, \mathbf{v}) \psi(t)} + \alpha(\mathbf{v}) \int d^3\mathbf{x}' dt' f(\mathbf{x} - \mathbf{x}', t - t', \mathbf{v}) \psi(t - t') \rho(\mathbf{x}', t'),$$

$$p(\mathbf{x}, t, \mathbf{v}) = \alpha(\mathbf{v}) \boxed{f(\mathbf{x}, t, \mathbf{v}) \Psi(t)} + \alpha(\mathbf{v}) \int d^3\mathbf{x}' dt' \boxed{f(\mathbf{x} - \mathbf{x}', t - t', \mathbf{v}) \Psi(t - t')} \rho(\mathbf{x}', t').$$

$G(\mathbf{x}, t, \mathbf{v})$

Convolution

Use Fourier transform

$$\Psi(t) = \int_t^\infty \psi(t) dt \quad \text{Prob of not scattering between } t=0 \text{ and } t$$

$$g(\mathbf{x} - \mathbf{x}', t - t', \mathbf{v}) = f(\mathbf{x} - \mathbf{x}', t - t', \mathbf{v})\psi(t - t'),$$

$$G(\mathbf{x} - \mathbf{x}', t - t', \mathbf{v}) = f(\mathbf{x} - \mathbf{x}', t - t', \mathbf{v})\Psi(t - t'),$$

$$p(\mathbf{q}, s) = \frac{\int \alpha(\mathbf{v})G(\mathbf{q}, s, \mathbf{v})d^3\mathbf{v}}{1 - \int \alpha(\mathbf{v})g(\mathbf{q}, s, \mathbf{v})d^3\mathbf{v}}.$$

$$p(\mathbf{q}, s) = \frac{\int \alpha(\mathbf{v})G(\mathbf{q}, s, \mathbf{v})}{1 - \int \alpha(\mathbf{v})g(\mathbf{q}, s, \mathbf{v})}.$$

Single
velocity

$$p(q, \omega) = 2\text{Re} \left[\frac{\sqrt{\frac{m\pi}{2kT}} \frac{1}{q} e^{z^2} \text{erfc}(z)}{1 - \sqrt{\frac{m\pi}{2kT}} \frac{1}{q\tau_c} e^{z^2} \text{erfc}(z)} \right] = 2\text{Re} \left[\tau_c \left(\frac{1}{1 - \sqrt{\frac{m\pi}{2kT}} \frac{1}{q\tau_c} e^{z^2} \text{erfc}(z)} - 1 \right) \right]$$

$$z(q, s) = \sqrt{\frac{m}{2kT}} \frac{1}{\tau_c} \frac{(1 + s\tau_c)}{q}. \quad (s = i\omega)$$

Same for 1, 2 and 3 dimensions

$$S_{xx}(\omega) = \frac{8L_x^2}{\pi^4} \sum_{n=1,3,\dots}^{\infty} \frac{p(q_n, \omega)}{n^4},$$

$$q_n = \frac{n\pi}{L_x}.$$

$$S_{vv}(\omega) = \omega^2 \sum_{n=\text{odd}} \frac{4L_x^2}{\pi^4 n^4} p\left(\frac{\pi|n|}{L_x}, \omega\right).$$

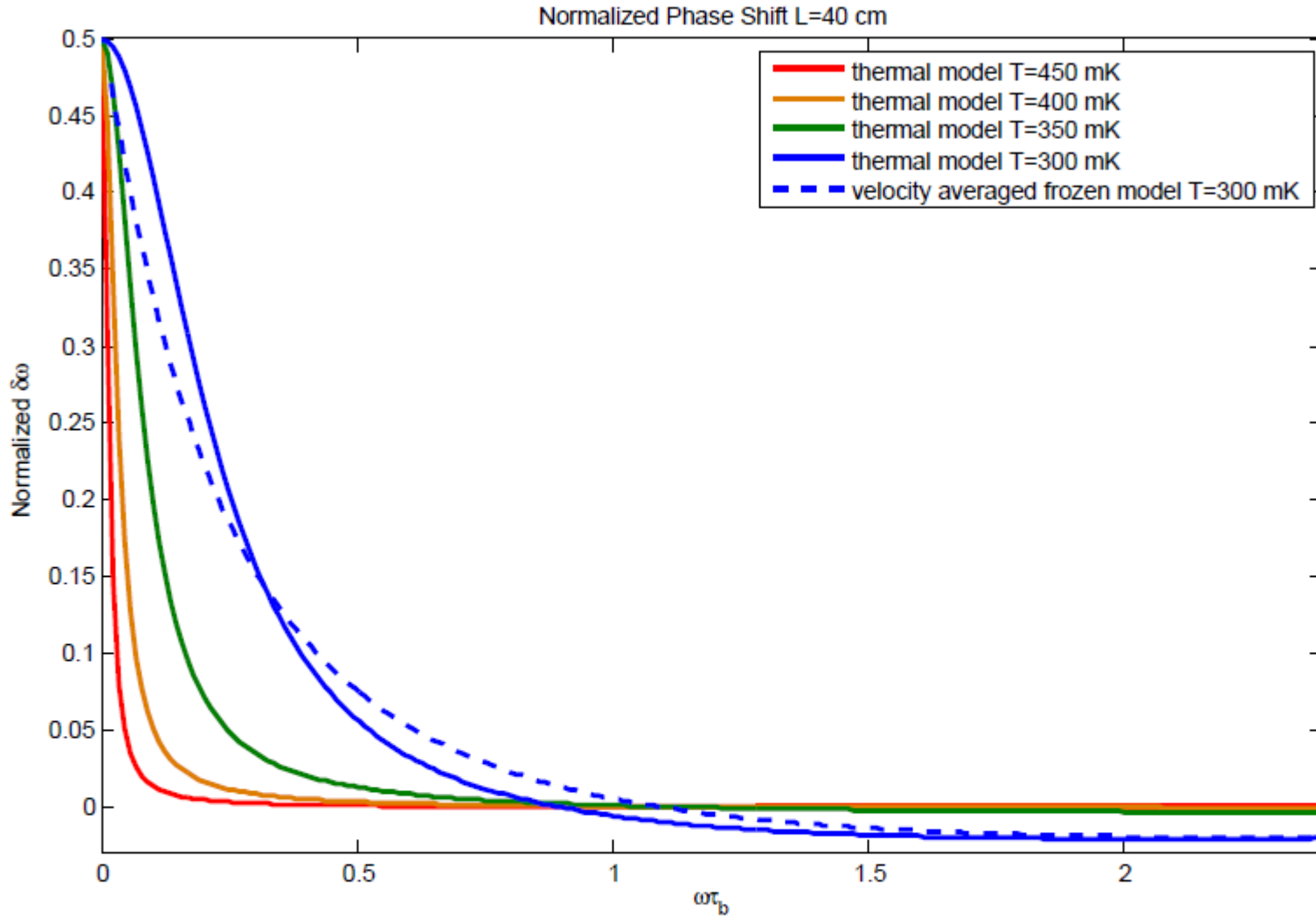


FIG. 7. The normalized spectrum of the linear in E phase shift for dilute ^3He dissolved in superfluid ^4He , with temperature as a parameter. All the solid curves are derived from the thermalization

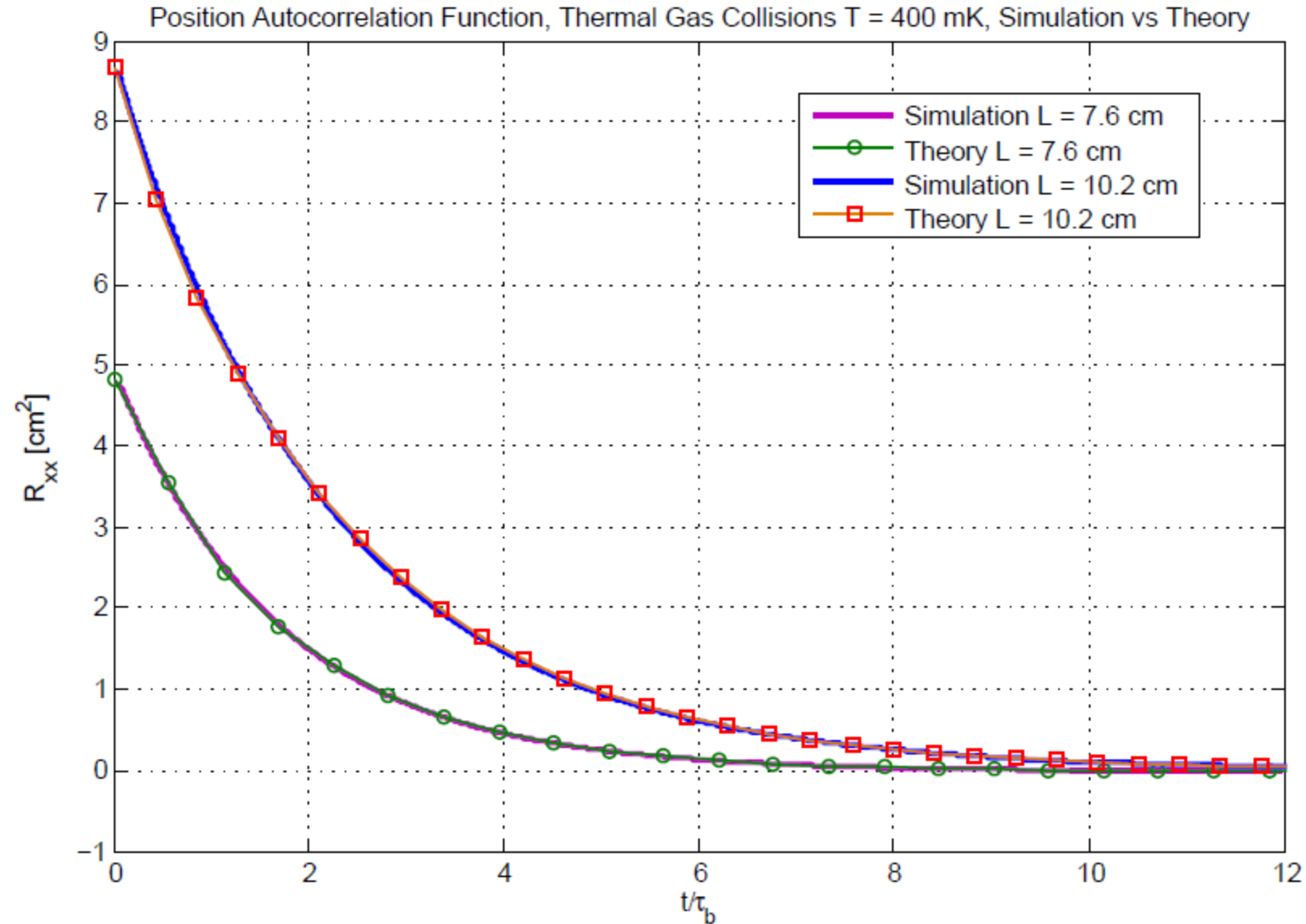


FIG. 10. The position autocorrelation function. The 3D Simulation is compared to thermalizatic theory. Good agreement is observed.

THEORY WITH THERMALIZING COLLISIONS He3

FALSE EDM vs. larmor frequency, T as parameter

